Multiple outflows in the bipolar planetary nebula MI-16: A molecular line study

Raghvendra Sahai[1,2*], A. Wootten[3], Hugo P. Schwarz[4], W. Wild[4]

1. Jet Propulsion Laboratory, California Institute of Technology, MS 169-506,4800 Oak Grove Drive, Pasadena, CA-9 1109

2. Dept. of Astronomy and Astrophysics, Chalmers University of Technology and University of Gothenburg, Gothenburg, S-41296, Sweden

3. National Radio Astronomy Observatory (NRAO), Edgemont Road, Charlottesville, VA 22903

4. European Southern Observatory (ESO), La Sills, Casilla 19001, Santiago 19, Chile

to appear in the 10 June, 1994 issue of

THE ASTROPHYSICAL JOURNAL

* Senior Resident Research Associate, National Research Council, National Academy of Sciences, Washington, D.C. 20418

ABSTRACT

Extensive observations of the molecular gas in the young, compact planetary nebula M 1-16 have been made, using the S wedish-ESO-Submillimeter Telescope. A map of the CO J=2- 1 emission shows that the molecular envelope contains both a slow and a fast outflow with expansion velocites of 19 km s^{-1} and >34 km s^{-1} respectively. The slow outflow is mildly elliptical while the fast molecular outflow is bipolar. This fast outflow is roughly aligned with the very fast outflows recently found in the optical while the long axis of the slow elliptical outflow is roughly orthogonal to the optical outflow axis. The kinematic time-scales for the CO fast outflow and the optical very-fast outflow agree closely, supporting the view that the former represents material in the slow outflow accelerated by the very-fast outflow. The kinematic signature of a disk expanding with about 15.5 km s^{-1} can also be seen in the CO J=2- 1 data. The mass-loss rate (a) for the slow outflow is 22.8x10-5 $M_O\,yr^{-1}$ and possibly as large as 9x1 $0^{-5}\,M_O\,yr^{-1}$, (b) for the fast outflow, is $\geq 5x10^{-6}\,M_O\,yr^{-1}$ and (c) for the very fast optically-visible outflow is $\approx$ 5x1 $0^{-7}\,M_O\,yr^{-1}$. The disk mass is =6x10-3 M_O. Grain photoelectric heating results in temperatures of 20-70K in molecular gas of the slow outflow, The $^{13}C/^{12}C$ abundance ratio in Ml- 16 is found to be 0.33, quite possibly the highest found for any evolved object.

Upper limits for the $^{18}O/^{16}O$ and $^{17}O/^{16}O$ ratios were found to be consistent with the values found in AGB stars. A search for other molecular speciesinM1-16 resulted in the detection of the high-excitation species HCN, CN, ^{13}CN, HCO^+, and $H^{13}CO^+$ and possibly N_2H^+. Both the HCO^+/HCN and CN/HCN line-intensity ratios are enhanced, the former by a very large factor, over the values found in the envelopes of AGB stars, probably as a result of enhancement of the CN and HCO^+ abundances due to photo-chemistry induced by the stellar UV. The CS J=2- 1, SiO J=2- 1, (v=0) and SiS J-6-5 lines were not detected to low levels. For the high-excitation molecules, adequate collisional excitation of rotational levels and survival against photodissociation by the UV radiation requires significant clumping of the molecular gas into clumps with H_2 densities -10^5 cm^{-3}. The IRAS fluxes of MI-16, assuming negligible contribution from line emission, imply the presence of about (1.7-0.4)x10^{-3} M_O of cool dust (temperature around 50K) and a smaller quantity, (2.7-3.1)x10-6, M_O of warmer dust (temperature around 125K) for a power-law emissivity index p=1-2.

The evolutionary nature of M 1-16 cannot be explained by existing single-star models of post-AGB evolution. The very high $^{13}C/^{12}C$ abundance ratio in M 1-16 suggests a possible evolutionary connection between M 1-16 and the rare class of J-type silicate-carbon stars which also have high $^{13}C/^{12}C$ ratios and are thought to be binary systems with accretion disks.

1. INTRODLJC'I'1ON

Planetary nebulae are thought to evolve from Asymptotic Giant Branch (AGB) stars after the latter undergo a short-lived (-2000 yrs or less) phase of rapid evolution termed the proto-planetary phase. Many objects believed to be in this phase show evidence of bipolar mass-loss occurring subsequent to the largely spherically-symmetric mass-loss during their AGB phase. The bipolar mass-Ioss during the protoplanetary phase may play a crucial role in the shape and shaping of bipolar planetary nebulae. A large number of planetary nebula have now been surveyed for CO emission (Huggins and Healy 1989), and many have been mapped with high spatial resolution (e.g. Bachiller et al. 1989a, b, Healy & Huggins 1990, Sahai, Wootten & Clegg 1990a, Bieging et al. 1991, Sahai et al. 1991, Bachiller et al. 1993). Such studies can constrain the history, structure and rate of the mass-loss occuring during the AGB and post-AGB phases, a knowledge of which is necessary for testing theoretical models of AGB/post-AGB evolution.

We report here extensive millimeter-wave observations of the compact planetary nebula Ml -16, made as part of our continuing study of molecular gas in planetary nebulae for probing the mass-loss which precedes and leads up to this phase of stellar evolution (e.g. Sahai, Wootten and Clegg 1993, Wannier and Sahai 1992). M 1-16 appears circular with a diameter of 3".6 in the 5 Ghz radio continuum (Aaquist and Kwok 1990). The optical nebula consists of a bright core of diameter 3" surrounded by a larger halo. Recentl y Schwarz (1992), using narrow-band optical imaging and long-slit spectroscopy, has discovered that M 1-16 is ejecting gas at very high velocities along a bipolar axis in a series of recent (≤1600 yr) mass-loss episodes. Estimates of the distancetoMl-16 by various authors cover a very large range, ranging from a maximum of 16.5 kpc (Shaw and Kaler 1989) to a minimum value of 1.8 kpc (Schwarz 1992). We have adopted a distance of 1.8 kpc which was proposed by Schwarz to be more plausible than the larger values and which is also more consistent with the data reported in this paper.

2. OIISERVATIONS

We observed M 1-16 in a number of millimeter-wave molecular lines, using the 15m S wedish-ESO-Submillimeter (SEST) telescope, at La Silla, Chile (Booth et al. 1989). 'l'he observations were made during several periods in 1990 April, 1991 February, June and October, and 1993 February, using cooled Schottky mixer receivers (tuned for SSB operation), with $T_{receiver} \approx$ 250-320K at $\lambda \sim 3$ mm and 700K at $\lambda \sim 1.3$ mm. We observed in the dual beam-switching mode, i.e. a rotating chopper wheel switched bet ween the source position and a reference position displaced alternate y east and west of the source by 12' in azimuth. The system was calibrated with the chopper-wheel method. Pointing, checked frequently by peaking on nearby stellar SiO J=2-1 (v=1) maser line sources, is estimated to be accurate (o within a few arcsec (3"). The data were recorded using onc or both of two Acousto· Optic Spectrometers, a high-resolution (43 kHz) one with a bandwidth of 85 MHz, and a]ow-resolution (690 kHz) onc with a bandwidth of 500 MHz during 1990-1991, and 1 GHz in 1993.

We detected CO J= 1-0 and 2-1 emission and made a map of the J=2- 1 emission with 11" (half-beamwidth) spacing. Lines from many other molecules were also observed towards the central position, and arc listed in Table 1. Line intensities are presented as main-beam brightness temperatures obtained by dividing the chopper-calibrated antenna temperatures by a measured beam-efficiency for small (planet-sized) sources. The beam-efficiency varies with frequency ranging from 0.77-0.74 at 90-115 GHz to 0.55 at 230 GHz. We determine a radial velocity of 50.5±1 km s^{-1} (V_{LSR}) from the CO lines, in good agreement with other CO measurements: Schwarz (1992) gives 48 and 49 km s^{-1} (V_{LSR}), while Huggins and Healy (1989) list 50 km S-l. Thus the radial velocity determined from CO lines improves significantly over the optical] y-determined value of 31.9±25 km s^{-1} (Schneider et al. 1983).

3. RESULTS

3.1. CO data

a) Spatial Distribution and Kinematics of the Mass outflows

The *slow and fast outflows*

The CO J= 1-0 and 2-1 profiles towards the center of M 1-16 display (i) a parabolic (or rounded) main component, and (ii) broad red and blue wings, indicating that the emission arises in a composite outflow consisting of a "slow" outflow and a "fast" component (Fig. 1). The expansion velocity of the slow outflow, V_{slow}, is determined by fitting an empirical line-shape function (e.g. Wannier et al. 1990) to the main component of the ^{13}CO J= 1-0 profile (Fig 1), and is found to be 19 km S-l, a factor 2 larger that derived from [0111], 10 km s^{-1} (Sabbadin, Strafella, and Bianchini 1986). The CO J=1 -O and 2-1 lines give slightly larger expansion velocities because of the more substantial presence of the high-velocity wings. These wings, not apparent in the lower signal-to-noise CO J=2- 1 spectrum taken with the NRAO12-m (Huggins and Healy 1989), are also seen in the CO J=1-0 and J=2- 1 spectra reported by Schwarz (1992). The full velocity range of emission covers V]s$_r$=17 to 85 km s^{-1}, as seen in a composite spectrum generated by averaging all CO J=2-1 spectra offset +/- 11" in RA and DEC from the center (Fig. 2), implying an expansion velocity of the fast outflow, V_{fast} >34 km s^{-1}. The latter is a lower limit because (a) the emission intensity in the line-wings gradually "tails off' into the noise at an expansion velocity >34 km s^{-1} and (b) the blue and red components arise in an outflow which is probably bipolar with its axis inclined at an angle to the line-of-sight (discussed below).

"l'he J=2-1 line profiles change systematically as a function of spatial offset from the center of the nebula (Fig. 3). "1'bus, whereas the line profile towards the center is largely symmetric about the stellar velocity (50 km s^{-1}), the line profiles offset from the center in selected directions are asymmetric. The spatio-kinematic structure of the molecular gas is displayed as a set of contour-maps of the CO J=2-1 emission intensity at different LSR velocities in Figure 4. Panels c and *d* showing emission within 10 km s^{-}I of the line-center are most representive of gas moving along the plane of the sky, and give a cross-sectional view of the envelope structure. In these panels, the emission contours, which arc centred

at the source-coordinates, are elliptical near the source-center, with the major axis of the ellipse aligned roughly NE-SW. The outer contours are similarly mildly elliptical, but also have small extensions perpendicular to (he major axis. The high velocity gas (panels *a* and *f*) is distributed asymmetrically about the source-center. The centers of the secondary blue and red emission components, seen in panels *a* and *f* are separated roughly along the NNW-SSE direction by about 10". 'I his spatial displacement of the blue and red high-velocity emission shows that the fast outflow is collimated along an axis which has the same P.A. as that of the very high-velocity optically-emitting gas seen by Schwarz (1 992), and orthogonal to the major axis of the elliptical structure seen in the slowly-expanding outflow. The bipolar axis of the CO high velocity outflow, like that of the optical very high velocity outflow, is inclined with the southern lobe directed towards us. CO emission was not detected in the extended optical lobes (labelled A in Schwarz 1992). The 1σ upper limits of 0.018 K and 0.07 K on the J=2-1 line intensity towards the northern ($\Delta\alpha, \Delta\delta$=- 16",44") and southern lobes (Act, $\Delta\delta$=1 6",-40") indicate gas column densities $<(1.4\text{-}4.6)\times 10^{17}$ cm^{-2} and $<(5.4\text{-}18)\times 10^{17}$ cm-2 respectively (taking the CO-to-H_2 abundance ratio, $f_{CO}=2\times10^{-4}$, and the line-width, ΔV=20 km s^{-1}) assuming LTE, and T_{exc}=20-100K

A collimating disk?

The elliptical contours seen at intermediate velocities in the CO J=2- 1 map suggest the possible presence of an equatorial density enhancement in the slow outflow similar to that seeninNGC3132 (Sahai, Wootten and Clegg 1990b), which maybe produced by an equatorial disk. Aspin et al. (1993) propose such a disk to explain their 3.6 μm image of Ml -16, showing a distinct elongation approximately perpendicular to the fast outflow. Since the fast outflow in M 1-16 is inclined to the line-of-sight by 45° (Schwarz 1992), an orthogonal disk must also be tilted by 45° along an axis running through the NE (11 ",1 1") and SW (-11 ",-11") positions. We find no evidence of disk rotation since there is no measurable difference in the mean velocity of emission between the NE and SW positions. If, however, the disk is expanding, then it should also show a "red-blue" spatial asymmetry, but opposite to that seen in the fast outflow, in the sense that disk gas north and west of center should be moving preferentially towards us, and south and west of center should be moving preferentially away from us. This expectation appears fulfilled from a comparison of the spectra at the (O, 11" = N), (-11 ",11" = NW) and (-11 ",0 = W) positions, where the central profiles (i.e. excluding the high-velocity emission) have a steep blue wing (at $V_{LSR}\approx$40 km s^{-1}), whereas at the diametrically opposite positions (O,- 11" = S), (11",-1 1" = SE), & (11",0= E), the central profiles have a steep red wing (at $V_{LSR}\approx$60 km s^{-1}). This effect is evident in a difference spectrum (hereafter referred to as the disk spectrum) (Fig. 5) generated by subtracting an average of the S, SE, and E spectra from an average of the N, NW, and W spectra, which clearly shows an "emission" peak 11 km s^{-1}bluewards, and an "absorption" peak at 11 km S-l redwards, of the stellar velocity. Correcting the 11 km s^{-1} expansion velocity of the disk gas for (he inclination gives a true expansion velocity of] 5.S kms^{-1}. Wc conclude that the slow outflow contains

an equatorial density enhancement, perhaps in the form of a disk, which may be collimating the fast outflow. Such a disk could either (a) a born-again disk formed from the redistribution of material in a planetary system (Sahai et al. 1991), or (b) produced by the gravitational capture of material around an unseen close companion from the precursor giant star slow wind (Morris 1987).

Taken together, the millimeter-wave and optical line data suggest that M 1-16 has a slowly expanding molecular envelope, a small fraction of which has been accelerated by the very fast wind, giving rise to the secondary blue and red CO components (Fig.6). This inference is supported by the close agreement between the expansion time-scale of the very fast optical outflow (1600 yr; Sch warz 1992) and the fast CO outflow (1500 yr, determined by dividing the ≈1O" separation of the secondary blue and red components by the difference in their mean velocities, 60 km s^{-1}). The spatial distortion of the envelope by the fast wind can be seen in the small elongations present to the NW and SE in the otherwise elliptical-shaped CO emission contours, Although the geometry and character of the molecular outflows in M 1-16 is similar to those seen in the more evolved planetary nebulae, NGC 3132 (Sahai, Wootten and Clegg 1990b) and IC4406 (Sahai et al, 1991), the latter do not show the presence of very fast optical outflows, indicating that the very fast outflow is transitory in nature (see $6).

b) Molecular Masses and Mass-Loss Rates

We first estimate the masses of the different kinematic components of the molecular gas in M 1-16 associated with CO emission in a simple way, assuming LTE and optically thin emission. Under these assumptions, the ratio of the integrated intensity of the CO J=1-O line, in the 31-69 km s^{-1} V_{LSR} range (observed with 45" resolution) to that of the CO J=2-1 line (convolved to **45"** resolution), equal to 1/1 .55, gives a characteristic (beam-averaged) excitation temperature of 14 K for the slow outflow. Summing up the CO J=2- 1 integrated intensity in the V_{LSR} velocity range31 **-69** km s^{-1}, we find the total number of CO molecules in the slow outflow to be 8.2x1051. The CO/H_2 abundance ratio, f_{CO}, in M 1-16 is not known, but is expected to be reduced below that found in the circumstellar envelopes of cool AGB stars such as IRC+10216 ($f_{CO}=6x10^{-4}$, Kwan and Linke 1982) because of photodissociation by stellar UV radiation. We will therefore assume for $f_{CO}=2 \times 10^{-4}$, guided by the value of $2x\ 10^{-4}$ found for the compact young planetary nebula NGC7027 (Jaminet et al. 1991). Then, the mass of the slow outflow is $M_{slow}=0.068\ M_O$. Similarly, for the fast outflow, $M_{fast}\approx 7.5x10^{-3}\ M_O$ calculated from CO 1-0 and 2-1 in the V_{LSR} velocity ranges 17-31 km s^{-1}, and 69-85 km s^{-1}. The disk mass, M_{disk}, is estimated from the sum of the (absolute values of) integrated CO 2-1 intensities in the "emission" component at -11 km s1 V_{LSR}, and the "absorption" component at 11 km s1 V_{LSR} in the disk spectrum (Fig. 5) to be $\approx 6.4x10^{-3}\ M_O$, where a scale factor of 2 has been applied to correct for disk emission around the stellar velocity which gets subtracted away by the differencing procedure. Since all masses scale as $(2x\ 10^{-4}/f_{CO})\ (1>/\ 1.8\ kpc)^2$, the ratios of the, masses inthe above components (slow

outflow, fast slow outflow, and disk) arc independent of D and f_{CO}, barring enhanced photodissociation in the fast outflow. Thus M_{slow}/M_{fast} is ≈10, and M_{disk}/M_{fast} is ≈1.

The average mass-loss rates *in the slow* and fast outflows (dM_{slow}/dt and dM_{fast}/dt) are estimated by dividing their masses by characteristic expansion time-scales (t_{exp}), derived from the observed source-sizes and outflow velocities. A gaussian deconvolution of the observed CO J=2- 1 brightness distribution at the line-center with the 22.5" beam gives a half-power size of 10.5" for the intrinsic distribution. The half-power radius is thus 1.4x1017 (1>/ 1.8 kpc) cm, giving t_{exp}≈2500 (D/1.8 kpc) yr, and $dM_{slow}/dt = 2.8x10^{-5} M_O yr^{-1}$. For the fast outflow, t_{exp}≈1500 yr, giving $dM_{fast}/dt = 5x10^{-6}$ $M_O yr^{-1}$. If this fast outflow is produced by the hydrodynamic action of the very fast outflow on the slow outflow, then $M_{v\text{-}fast} V_{v\text{-}fast} \approx M_{fast} V_{fast}$, and $dM_{v\text{-}fast}/dt\, V_{v\text{-}fast} \approx dM_{fast}/dt\, V_{fast}$, where v-fast refers to the very fast outflow. Since Schwarz (1992) estimates $V_{v\text{-}fast}$ ≈350 km S-l, WC find $M_{v\text{-}fast} \approx 7x10^{-4}$ M_O, and $dM_{v\text{-}fast}/dt \approx 5x10^{-7} M_O yr^{-1}$. The masses and mass-loss rates are lower limits because of the conservative nature of our assumptions regarding the CO excitation and opacity.

A more sophisticated estimate of dM_{slow}/dt has been made by using an excitation/ radiative transfer code (Sahai 1990) for spherically symmetric envelopes to fit the CO data, since the non-spherical components in the Ml-16 molecular envelope affect the main component emission (i.e. which arises in the largely spherical slow outflow) only to a small extent, The line-center intensity of the main component is least affected, whereas the line-shape (i.e. the roundedness) is most affected, The CO is collisionally excited since there is very little flux at near-lR wavelengths (see Fig. 4 of Schwarz 1992) for radiative excitation. The radial distribution of CO, determined by photodissoeiation by the interstellar UV, is calculated according to the prescription given by Maroon et al. (1988). The inner radius is taken to be 1.8" from the 5 GHz VLA map of M 1-16, A power-law is assumed for the unknown radial kinetic temperature distribution, $T_{kin}(r)$. Acceptable fits to the data require a T_{kin} ranging from ≈70K at the inner radius of 4.8x1016 cm to ≈20K at 3.5x1017 cm, which is the radius where the CO abundance has fallen to half its initial value. Both J=1-0 and 2-1 are found to be subthermally excited in large regions of the envelope which contribute to the observed emission. q'bus, the model values of dM_{slow}/dt are higher than those derived assuming LTE at a beam-averaged temperature of 14 K. We find dM_{slow}/dt to be larger than $\approx 5x10^{-5} M_O$ yr l in order for the CO J=2 level to be sufficient] y populated, and the observed J= 2-1 to 1-0 line intensity ratio (≈3.9) to be reproduced. Models in the range of $dM_{slow}/dt = (5.5\text{-}8.7)x10^{-5} M_O yr^{-1}$ for $f_{CO} = (1.8\text{-}1)x10^{-4}$ fit the data (Table 2), which, in addition to the SEST observations, includes the J=2-1 line observed with the NRAO12-m telescope (higher mass-loss rates, together with f_{CO} <10-4 can also fit the data). The model line-shapes, with maximum intensity at the line-center, are in moderate agreement with the observations. A more detailed comparison of models and data is not sought in the line-wings, due to the more significant affect of emission from the. bipolar outflow component at velocities near and around the expansion velocity of the slow outflow. We discuss later (§ 3.3) the possibility of significant clumping of the gas in the slow outflow, allowing us (o fit the

CO J=2-1 to 1-0 ratio with a lower average mass-loss rate. However, the lower limit (o dM_{slow}/dt remains 2.8x 10-5 $M_O\,yr^{-1}$ (with $f_{CO}=2\times10^{-4}$), as derived in §3.1 b. Noting that very few red giant mass-loss rates exceed $10^{-4}\,M_O\,yr^{-1}$ [only in two cases have larger mass-loss rates been derived, $1.7\times10^{-4}\,M_O\,yr^{-1}$ for the protoplanetary nebula CRL2688 (Truong-Bach et al. 1990) and $3\times10^{-4}\,M_O\,yr^{-1}$ for the compact young planetary nebula NGC7027 (Deguchi et al. 1990)], it is unlikely that the distance to M 1-16 is much larger than 1800 pc.

What physical processes maintain the molecular gas in M 1-16 at the temperatures required by the above modelling? Using new JHKL photometry obtained with the ESOIR photometer (see Table 4), we find that the drift velocity of the dust (with respect to the gas), V_{drift}, is only ≈0.06 km s^{-1}. Hence the frictional heat input to the gas is negligible in the M 1-16 envelope, unlike the case of AGB star CSEs, where it is the dominant source of heating. We therefore consider the relative importance of alternative gas-heating mechanisms in the Ml-16 envelope: heat-exchange between the dust and gas, and the photoelectric emission from dust grains duc to the far-UV stellar radiation[1]. Using standard formulae for the heating rate due to grain photoelectric heating (dq_{pe}/dt) (Hollenbach et al, 1991) and gas-grain collisions $(dq_{g\text{-}d}/dt)$ (e.g. Deguchi et al. 1990), we find

$$(dq_{pe}/dt)/(dq_{g\text{-}d}/dt) \approx 9\times10^{3}\,(G_0\,e^{-\tau}/500)\,(L_*/100\,L_\odot)(a/0.1\mu)(\rho_d/2\ g\ cm^{-3})$$
$$\times\,([T_d-T_k]/1\ OK)\,(dM/dt\,/\,10^{-4}\,M_O\,yr^{-1})(V_{drift}/0.1\ km\ s^{-1})^{-1}$$

where G_0 is the factor by which the unattenuated stellar far-UV radiation exceeds the value for the average interstellar field, $e^{-\tau}$ is the attenuation of this radiation in the molecular outflow, L_* is the stellar luminosity, a and ρ_d are the grain radius and material density, T_d and T_k are the dust and gas temperatures, respectively. Inserting values of the various physical parameters appropriate for M 1-16, in the above equation, the ratio $(dq_{pe}/dt)/(dq_{g\text{-}d}/dt)$ is very large (several hundred), implying that the grain photoelectric effect is the primary mechanism by which gas is heated in the M 1-16 molecular outflow.

3.2. ^{13}CO, $C^{18}O$, & $C^{17}O$ data: isotope ratios

'I'he mean ratio of the J=1-O $^{13}CO/^{12}CO$, $H^{13}CO^+/HCO^+$ (Fig. 7a), and $^{13}CN/CN$ (Fig. 7c, 7d) integrated intensities is 0.32, suggesting that the $^{13}CO/^{12}CO$ abundance ratio is very large, at the high end of the range of values found in AGB CSEs. In order to derive the abundance ratio from the intensity ratio, we must correct for any optical-depth effects (general] y for the ^{12}C-substituted species) and the slightly different frequencies of the ^{12}C and ^{13}C-substituted lines. The I I $^{13}CO^+/HCO^+$, $^{13}CN/CN$, and $^{13}CO/^{12}CO$ abundance ratios are found to bc 0.33, 0.32, and 0.35 respectively. The abundance ratios are close to the line-intensity ratios, since the lines are optically thin (e.g line-center optical depth, τ_o = 0.1, 0.19[2], and 0.03 at $r=1.5\times10^{17}$ cm for the 1-O lines of HCO^+, CN, and CO respectively). An

[1]: Ibis mechanism also operates in the outer layers of the molecular cnvc.lope, which arc permeated by the interstellar UV radiation

[2]the optical depth of the CN line given here is actually a sum of the optical depths of 9 hyperfine components, thus the optical depth of any single component is significantly smaller than 0.19

average of the results from the three molecules gives a $^{13}C/^{12}C$ abundance ratio of 0.33.Such a high carbon-isotope ratio has important implications for [he evolution of M 1-16 (which wc discuss in §6). We believe that our derived $^{13}C/^{12}C$ ratio is reliable, since three different molecular species give almost the same value for this ratio. Only upper limits were obtained for the $C^{17}O$ and $C^{18}O$ lines. These upper limits imply that the $^{16}O/^{17}O$ and $^{16}O/^{18}O$ abundance ratios are >70, and >130, respectively. These are consistent with the typical values of these ratios observed in AGB envelopes ($^{16}O/^{17}0$=250-1000, $^{16}O/^{18}O$≈300-1250, e.g. Wannier and Sahai 1987, Kahane et al. 1992).

3.3. Circumstellar chemistry in MI-16

We have detected emission in the 1-O transitions of HCN, CN, HCO^+, $H^{13}CO^+$, ^{13}CN and possibly N_2H^+. Sensitive upper limits were set on the SiO J=2- 1 (v=0), CS J=2- 1 and SiS J=6-5 lines. Empirical fits to the HCO^+ and $H^{13}CO^+$ (Fig. 7a) profiles give outflow velocities of about 27 km s^{-1}, intermediate between that found for the slow and fast CO outflows. The HCN line (Fig. 7b) contains emission from 3 hyperfine (hf) components. After deconvolving the hf-structure (assuming each component to be optically thin and proportional to its relative intensity (RI), the HCN profile (not shown) gives an outflow velocity of about 25 km s-1, The ^{12}CN and ^{13}CN transitions are split up into many hf-components but the relatively low signal-to-noise does not allow deconvolution of the hf-structure. In the case of ^{12}CN, the hf components are clustered in two frequency ranges 113488-113520 MHz, and 113123-113191 MHz: the spectrum (Fig.7c) clearly shows the blended components belonging to the higher frequency set, whereas for the lower frequency set, which has a combined RI half that of the fomer, the emission is only weakly visible. In the case of ^{13}CN (Fig. 7d), the usable spectral passband covered 13 out of a total of 15 hf-components, spanning the frequency ranges 108631-108659 MHz (total RI=48.5%) and 108780-108796 MHz (total RI=43.7%) (Gerin et al. 1984). We have co-added the regions of the spectrum containing the lower frequency set (average frequency, <v>=108648 MHz) and the higher freqency set (<v>=108784 MHz): the higher signal-to-noise ratio spectrum (labelled "composite") clearly shows that ^{13}CN is present in M 1-16.

We have calculated the abundances of the observed molecular species, using Eqn. (1) of Sahai and Wannier (1992), assuming a fixed excitation temperature, T_{ex} =14 K for all species. The relative abundances of HCN, CN, HCO^+, and N_2H^+ are insensitive to the precise value and variation of T_{ex}, because their fundamental rotational transition lie at roughly similar frequencies, giving similar rotational partition functions. The inner radius is, as for CO, taken to be equal to 1".8[3]. The outer radius for each species is set by photodissociation by the interstellar UV, and depends on its particular photodissociation rate and the shielding provided by dust, A quantitative estimate of the radial distribution of each species taking into account the various production and destruction mechanisms, is deferred to another paper.

[3]for an optically-thin line the model intensity is proportional m the total number of molecules (which increases linearly with radius) , and is therefore modestly sensitive to the value. of the inner radius

Here we simply assume the same fixed outer radius for all species, which wc set equal to 1,5x1017 cm, half that of the CO half-abundance radius. The derived abundances, f_{mol} (Table 3), can be scaled to other values of the rotational excitation temperature, the outer radius of the envelope, and the mass loss rate, using the following proportionalities (a) $f_{mol} \propto T_{ex}^{a}$, where a≈ 0.75, 0.69, and 0.1 respectively, for species in which the 1-O, 2-1, or 6-5 transition was observed, for 15K<T_{ex}<60K, (b) $f_{mol} \propto (R_{out})^{-2}$, and (c) $f_{mol} \propto (dM/dt)^{-1}$. We find the HCO^+/HCN and CN/HCN abundance ratios in M 1-16 (0.9 and 8.5 respectively) to be significantly larger than those found in the CSEs of AGB stars and preplanetary objects (e.g. CRL2688), and similar to those found in the evolved planetary nebulae IC4406 and NGC6072 (e.g. 'l'able 2 of Cox et al. 1992). The enhanced HCO^+/HCN and CN/HCN abundance ratios in M 1-16 (compared to AGB CSEs) probably result from: (a) production of HCO^+ and CN in the inner layers of the CSE due to chemistry driven by shocks and the stellar UV, and (b) a decrease in the abundance of HCN due to photodissociation by the stellar UV[4].

Although the relative molecular abundances are not very sensitive to T_{ex}, it is important to understand two related issues. The first issue relates to the excitation of the high dipole-moment (compared to CO) species such as HCN, CN, and HCO^+. Whereas in an AGB CSE the rotational lines of such species are usually excited by the infrared radiation from the central source, in M 1-16 this source of excitation is very weak, resulting in strongly subthermal excitation. Using the radiative transfer/ excitation model described in §3.1 we find that even with dM/dt as large as 8.7x10-5 $M_O\,yr^{-1}$, the gas density falls rapidly (as r^{-2}) below the critical density for these species (typically $10^6\,cm^{-3}$) at radii larger than ≈0. 15". Thus in the 1.8 to few arcsec radial region, which contributes dominantly to the CO emission, T_{ex} ≈(8-2.8) K for the 1 ICN, CN, and HCO^+ lines, not much larger than that of the microwave background. Consequent] y, it is not possible to reproduce the observed Ii ne intensities for the high-dipole moment molecules. The second issue relates to the survivability of these molecules in the harsh photoionizing radiation from the central star. Howe, Millar and Williams (1992) find from time-dcpcndent chemistry calculations in an interacting-winds planetary nebula model, that most existing molecules (except H_2 and CO which are mutually- and self-shielded against photodissociation) in the AGB envelope are destroyed in about ≈100 yr from the time when the central star reaches a T_{eff} ≈30,000K. In the unshocked regions of the slow outflow, all polyatomic species are destroyed very rapidly. In a thin, shocked region at the inner boundary of the slow outflow (r≈10^{16} cm), a few small hydrogenated molecules and molecular ions such as CH^+, CH_2^+, CH_3^+, CH, CH_2, and NH attain abundances typically of fewx 10^{-9} at post-shock times≈100 yrs, for a stellar luminosity of $10^3\,L_O$. These abundances decline rapidly with radius and time. Hence, even though the luminosity ofM1-16 is a factor 8 lower than the model, we can safely conclude that the much larger observed abundances of HCN, CN and HCO^+ (see 'l'able 2) require that some mechanism protect and/or regenerate these molecules.

[4] see Cox et al. (1992) for a more derailed discussion of chemistry

4. A Clumpy Structure for the Molecular Gas

Noting that clumping is probably necessary in order to explain the CO emission from within the ionized regions of well-resolved planetary nebulae like IC4406 (Sahai et al. 1991) and NGC3 132 (Sahai, Wootten and Clegg 1990b), wc suggest that a possible solution to the problem of exciting high-dipole moment molecules such as HCN, CN, and HCO^+ in M 1-16 is to distribute the gas in small, dense clumps with H_2 densities ≈ 105-106 cm^{-3}. It is possible, but unlikely that such clumping arises as a result of the action of the highly-collimated very high-velocity outflow upon the slow outflow, specially along directions well removed from the bipolarity-axis, It is more probable that the clumping is intrinsic to the mass-loss process which produced the slow outflow in M 1-16.

We now examine the time-evolution of a typical clump. Assuming typical values for the temperature, radius, and density (1 OOOK, 10^{13} cm, and 10^{12} cm^{-3}, respectively) of a spherical clump at ejection from the star, which expands at the sound speed in the clump, $v_s(t) \approx 0.08 \sqrt{T_k(t)}$ km s^{-1}, we find that the clump kinetic temperature $T_k(t)$, radius $\delta r(t)$, and density n(t), evolve roughly as $T_k(t) \approx 1000\ t^{-2\alpha/(2+\alpha)}$ K, $\delta r(t) \approx 10^{13}\ t^{2/(2+\alpha)}$ cm, and $n(t) \approx 10^{12}\ t^{-6/(2+\alpha)}$ cm^{-3} where t is the elapsed time in years, and α takes values between 2 (adiabatic cooling only) and 0.5 (substantial heating) (e.g. Bergman, Carlström and Olofsson 1993), Thus, in the case of M 1-16, such evolution would produce clumps of temperature and density of51 K and 1.8x 10^4 cm^{-3} for α=0.5, and 0.6K and 1.5x10^7 cm^{-3} for α=2, at a typical radius of 10^{17} *cm* (t=1750 yr) in the slow outflow. With an intermediate value of α=0.8, wc can get a clump temperature of $14\,K(r/10^{17}\,cm)^{-0.57}$, and density of 1.3x1 $0^5(r/10^{17}\,cm)^{-2.1}$ cm^{-3}: note that this choice of *a* preserves the inverse-square density distribution (applicable to a smooth outflow at a constant mass-loss rate and constant expansion velocity) and the radial kinetic temperature distribution used in the radiative transfer/ excitation code used in § 3.1 b. The factor 25 increase in the density increases the collisional excitation sufficiently for producing the observed emission from the high dipole-moment molecules. The clump size (with α=0.8) is $4x\ 10^{15}$ $(r/l\ 0^{17}\,cm)^{0.71}$. Thus, the physical properties of the deduced clumps in the M 1-16 molecular outflow are similar to those of the very small (1") condensations found in NGC7293 (e.g. Vorontsov-Velyaminov 1968) and discussed by Dyson et al. (1989). It is not clear whether the patchy appearance of CO emission (on scales of - 1017 cm) seen directly towards various planetary nebulae mapped with high-resolution (1 2") (e.g. NGC2346: Bachiller et al. 1989, NGC6781: Bachiller et al. 1993) results from an aggregation of the type of small clumps wc deduce to be present in M 1-16, or whether it results from fragmentation of the slow outflow.

Clumping will lead to a lower net photodissociation of the high-dipole moment molecules. Howe, Millar and Williams (1992) find from a time-dependent chemistry model of clumped molecular gas in a planetary nebula that observable amounts of some polyatomic species may exist in clumps with physical proper-tics similar to those described above. The CN/HCN abundance ratio in these models increases with the time elapsed from the onset of clump photoionization as well as with the distance from

the central star: large values of the CN/HCN ratio (as observed in M 1- 16) are produced for t ≥ 3000 yr, and a radius > 1.6 x10^{17} cm (for an expansion velocity of 15 km s^{-1}). Since the molecular envelope of M 1-16 extends from about 4.8x1016 cm to about 3 x1017 cm and the corresponding expansion times are 850-5250 yr, we conclude that our observations of CN and HCN are probably consistent with the clumpy chemical evolution models of Howe, Millar and Williams (1992). However, specific modelling tailored to the physical parameters ofM1-16 (luminosity, expansion velocity, mass-loss rate) will be necessary to firmly establish if chemistry in clumps, evolving under the influence of UV irradiation, can explain the abundances and abundance ratios of CN, HCN, and HCO^+ in M 1-16.

5. IRAS data: Dust emission

The IRAS measurements show that the far-infrared emission of M 1-16 peaks in the 60-100 μm range, indicating significant emission at λ>100 pm, Using the two-component dust model described by Sahai et al. (1991), we find the temperatures and masses[5] of these components to be 53K, 4.3x10^{-4} M_O and 131K, 3.1x10-6 M_O for p (emissivity power-law index)=l, and 41K, 1.7x10-3 M_O and 114K, 2.7x 10^{-6} M_O for p=2, assuming a 60 μm dust emissivity of 150 cm^2 g^{-1}. Most of the stellar luminosity is re-emitted in the far-IR as thermal emission from dust grains since the near-IR photometry shows a sharp decrease in the flux at λ<10 μm. Integrating the emission from the model dust components over all frequencies, we find that the total luminosity of M1-16 is ≈120 L_O, validating Schwarz's (1992) estimate obtained by multiplying the integrated flux density by a factor 1.5 to correct for the emission at long wavelengths. Although our modelling of the dust emission is simplistic, it shows that a substantial mass of cool dust exists in M 1-16, most probably associated with the cool molecular gas seen in CO emission. The total mass of gas in the nebula, which scales linearly with the outer radius of the envelope, cannot be determined from the present observations, The radius at which the CO abundance decreases to l/c of its initial value due to photodissociation (4 x10^{17} cm from our CO modelling) sets a lower limit to the outer radius, implying that the molecular mass M_g≥0.56 M_O (dM/dt / 5.5 x 10^{-5} M_O yr^{-1}). Hence the gas-to-dust ratio is M_g/M_d ≈ 500. This ratio is uncertain because we do not know (1) how far the envelope extends beyond 4 x10^{17} cm, and (2) if substantial quantities of cold dust (T_d<1 SK) observable only at very long wavelengths (e.g. 800 pm), arc also present in the envelope.

6. The Nature of MI-16 and its Outflows

The relatively strong molecular line emission from M 1-16 shows that it has a largely intact circumstellar envelope, presumably from the red giant phase, supporting its identification as a very young planetary nebula. Let us assume that at time t=0, the red giant mass-loss (i.e. the slow outflow) effectively ceases, and at t=t_1, the ionisation "switches" on. "l'he ionisation front will cat its way into the expanding red giant outflow at some finite speed (V_{ion}). Thus the radius of the ionised nebula, seen in

[5]Dust masses scale as the distance-squared, and inversely as the emissivity

the radio continuum, at a time $t=t_{evol}$, will be at a radius, $R=V_{exp}t_1 + (V_{ion}+V_{exp})(t_{evol}-t_1)$. The expansion age of the ionised nebula, t_{exp}, given by R/V_{exp}, is $t_{evol}+(V_{ion}/V_{exp})(t_{evol}-t_1)$, and is estimated to be 8S0 yr from the 1 ".8 radius of the radio image and 19 km s^{-1} expansion velocity. Hence the evolutionary age, t_{evol}, and the time elapsed since (hc onset of ionisation, $t_{ion}=t_{evol}-t_1$, is <850 yr. Comparing this with the expansion ages of the 3 optical lobes comprising the very high-velocity optical outflow (1600, 1050, and 740 yr), wc conclude that at least the older of the two were produced before the formation of the (ionised) planetary nebula. The chemical composition of the molecular gas in the CSE of M 1-16 is different from that of a CSE in a red giant star. The difference is probably due to the evolution of the central star from a cool red giant to a white dwarf emitting copiously in the UV.

However, Schwarz (1992) pointed out that if M 1-16 is a young planetary nebula evolved from an AGB star, it is dificult to explain its very low luminosity (120 $L_\odot$) compared to a typical AGB star (typically (0.5- 1)x10^4 $L_\odot$]. In addition, in order to radiatively drive the slow CO outflow in Ml -16 (e.g. by radiation pressure on dust grains, as in typical AGB stars), one would require a luminosity of at least ~10^4 $L_\odot$ (e.g. the momentum in the slow outflow, $dM/dt \times V_{slow} \geq 3.6\times10^{27}$ g cm S^{-2}, whereas $L/c=1.6\times10^{25}$ g cm S^{-2} in Ml-16). If one infers, therefore, that the luminosity of the star has dropped abruptly since the bulk of the observed outflowing mass was ejected, one runs into an inconsistency with theoretical evolutionary tracks for post-AGB stars. Using our estimates of the age (<850 yr) and luminosity (120 $L_\odot$), and A spin et al's (1993) estimate of the effective temperature for the central star ($T_{eff}=3.4\times10^4$ K), ***we*** have tried to place Ml-16 on the evolutionary tracks of post-AGB stars or PNN (Planetary Nebula Nuclei) computed by Wood and Faulkner (1 986, hereafter WF), but are unable to find a fitting track for the range of PNN masses considered by WF (0.60-0.89 $M_\odot$). If, from the small evolutionary age of ≤850 yr and low central star T_{eff}, we infer that M 1-16 is a very young planetary nebula (in the evolutionary sense), then we cannot explain its very low luminosity. If we infer that its low luminosity is because of rapid evolution of a massive PNN, then wc cannot explain its low T_{eff}. A spin et al. derive T_{eff} by comparing their observed (He] λ=2.058 μm) /(Br-γ 2.166 μm) line intensity ratio with theoretical models (Doyon, Puxley and Joseph 1992). Although the HeI/Br-γ ratio saturates at a value of 0.8 (assuming a Galactic helium abundance) for $T_{eff} \geq 4\times10^4$ K, A spin et al's observed value, 0.45±0.05, is significantly lower, making it very unlikely that the low T_{eff} results from measurement uncertain y. We conclude that M 1-16 does not fit the post-AGB tracks of single stars.

The obvious alternative for explaining the nature of M 1-16 is that the central star is a binary. Schwarz (1992) suggested that a binary central star with mass-exchange, in M 1-16 could have produced the extensive mass-loss, without having to invoke a large luminosity. This is an attractive hypothesis, since a binary star could provide (a) a means of explaining the bipolarity of the very fast optical ouflow, and (b) the energy to power these outflows (the present stellar luminosity of M 1-16 being too low to provide the momentum in the very fast outflow). Morris (1987) has proposed a modelin which the slow outflow from a red giant is captured into a large accretion (and/or excretion) disk by a main-sequence Or

compact companion: the disk powers a fast collimated outflow via its rotational energy. We therefore compare the kinetic energy in the very fast outflow (1/2 $M_{v\text{-}fast}(V_{v\text{-}fast})^2$=8.6x$10^{44}$ erg) with the rotational energy in our proposed disk, E_{rot}. If the disk rotated rigidly, the maximum rotational speed of the disk (obtained at the disk edge) would have to be 160 km s^{-1}, orders of magnitude larger than that possible from Keplerian motion around any reasonable central mass. If the disk gas was in Keplerian rotation around a companion with mass M_c»M_d then E_{rot}=G$M_c M_{disk}$/R, where R is the disk radius. Adopting Aspin et al's. (1993) value for R of -1.5" (4x10^{16} cm at 1.8 kpc), wc find E_{rot}=4.4x10^{40} (M_c/1$M_\odot$) (1.8 kpc/D) erg, insufficient for driving the very fast outflow by many orders of magnitude.

If binary gravitational interaction drove the slow outflow (obviating the need for a large luminosity), then the orbital plane for mass-ejection would have to be inclined at a large angle (=i) to the line-of-sight, because the slow CO outflow as well as the ionised nebula show near circular symmetry on the sky. The symmetry of the very fast bipolar outflow, which should be orthogonal to the orbital plane, argues for i≈45°. However, a highly-flattened configuration of outflowing gas, with i between 45° and 90°, should show large velocity shifts of the main line profile, as the beam moves from the side of the disk tilted towards us, to the side tilted away from us. Such velocity shifts are not observed in the data (see Fig. 3). We therefore think that it is unlikely that the slow outflow arises in a flattened distribution resulting from binary gravitational interaction. Acoustic waves provide an alternative mechanism for driving the slow outflow (Pijpers and Habing 1989, Pijpers, Hearn and Habing 1990).

Ml-1 6 is not unique in presenting the problems pointed out above. A closely analogous case is that of the Boomerang nebula (IRAS 12419-5414) (e.g. Wegner and Glass 1979) which is a visibly bipolar nebula, sharing many similarities with M 1-16. It has a mass-loss rate (deduced from CO observations) of (2-3) x10-5 $M_\odot$ yr^{-1}, ouflow velocity 22 km s^{-1}, an enhanced $^{13}C/^{12}C$ ratio of about 1/5, and a central star with T_{eff}=7000K and luminosity of 80-80010, for a distance D=0.8-2.5 kpc (Bujarrabal and Bachiller 1991), The high mass-loss rate, comparable to that in M 1-16, implies (assuming radiatively driven mass-loss) AGB luminosities >fewx10^4 $L_\odot$, again leading to an inconsistency with evolutionary tracks of post-AGB stars. Bujarrabal and Bachiller (1991) suggest that the low luminosity of the Boomerang is due to a low-mass (initial mass < 1$M_\odot$) progenitor, but do not address the problem of how it ejected mass at such a large rate. It would be of interest to sensitively map the Hα and CO emission from this object. Since the central star in the Boomerang is less evolved the central star in Ml-16, a search for a high velocity bipolar outflow in the Boomerang nebula will address the issue of precisely when, during the post-AGB phase, the bipolar high-velocity flow is generated.

A clue to the evolutionary nature of M 1-16 is provided by the high $^{13}C/^{12}C$ abundance ratio (0.33) in M 1-16, which can only be reached in equilibrium CNO-nucleosynthesis. A second signature of substantial CNO-processing is a high N-abundance, inferred to exist in the very high-velocity outflow (Schwarz 1992). High $^{13}C/^{12}C$ ratios, in excess of 0.1, arc found in (1) oxygen-rich CSEs, such as OI 1231.8 (Morris et al. 1987), and (2) in the rare class of carbon stars known as J-type (e.g. Y CVn or

T Lyr) (Lambert et al. 1986). Although nebular abundances have apparently not been determined in M 1-16, our detection of CN and HCN, coupled with the lack of SiO emission, suggest that the slow outflow in M 1-16 is carbon rich. Lambert et al. (1990) sketch reasons to suppose that the cool J-type carbon stars represent evolved examples of the early R stars which also show ^{13}C-rich envelopes, without the s-process element enhancement typical of normal carbon stars (Dominy 1984). They note that these stars would then have much lower luminosities than normal AGB carbon stars. Richer (198 1) found that the two least luminous carbon stars in his LMC sample were J-type stars, one of them quite cool. Bessell, Wood and Lloyd Evans (1983) found a similar object in NGC419 in the SMC. All three of these objects have bolometric magnitudes one or more magnitudes fainter than normal cool carbon stars. The ^{13}C enrichment, possible carbon-rich nature, and the low luminosity of M 1-16, suggest that, like a J-type carbon star, it has evolved from an R star.

A small fraction of J-type carbon stars display a 10 μm silicate emission feature (hereafter referred to as silicate-carbon stars), indicative of oxygen-rich material. (Willems and de Jong 1986, Lambert et al. 1990), Noting that the similarity in the frequency of binary occurrence for R stars and normal K giants implies that the formation of an R star is probably independent of the presence of a companion, Lambert et al. (1990) have extended their evolutionary scenario for J-stars to the silicate-carbon stars. In their model a low-mass main-sequence companion captures some of the mass lost from the giant progenitor of the J-type star into an accretion disk, which produces the silicate emission (Lloyd Evans 1990). Since a binary ongin has been shown above to be an attractive and perhaps even necessary hypothesis for Ml -16, it is tempting to speculate that M 1-16 has evolved from a silicate-carbon star. Unfortunately, a high-resolution 10 μm spectum does not exist for Ml -16 for testing this hypothesis, Also, no CO emission has been detected from any silicate-carbon star to very low-levels (Deguchi, Nakada and Sahai 1990, Little-Marenin et al. 1993), indicating the possible lack of extended envelopes with $dM/dt \geq$ few x 10-7 $M_O\ yr^{-1}$. However, if silicate-carbon stars are significantly less luminous than AGB stars, then their mass-loss rates maybe much higher, since the circumstellar gas lacking significant dust frictional heating, may be sufficiently cold to result in a non-detectable level of CO emission. As the primary star in these objects evolves towards higher temperatures, grain-photoelectric heating becomes effective in heating the gas, giving rise to detectable CO emission as seen in M 1-16.1 lence it is possible that M 1-16 was a silicate-carbon star before evolving into a planetary nebula.

7. SUMMARY

We have made extensive observations of the young, compact planetary nebula Ml -16 in the millimeter-wave lines of CO and other molecules. Our conclusions are summarised below.

1) The CO data show that the M 1-16 molecular envelope contains both a slow and a fast outflow, with expansion velocites of 19 km s^{-1} and >34 km s^{-1}, respectively. The slow outflow is mildly elliptical whereas the fast molecular outflow is bipolar. This fast outflow is roughly aligned with the very fast

bipolar outflows seen optically, while the long axis of the slow elliptical outflow is roughly orthogonal to the optical outflow axis.

2) The kinematic time-scales for the CO fast outflow and the optical very-fmt outflow arc similar, suggesting that the former represents material in the slow outflow accelerated by the very-fast outflow.

3) The kinematic signature of a disk expanding at $\approx$15.5 km s^{-1} can be seen in the CO data. This disk, which may collimate the very-fast outflow, has insufficient rotational energy for powering the latter.

4) The mass-loss rate for (a) the slow outflow is 22,8x10-5 M_O yr^{1}, and possibly as large as $9x10^{-5}$ M_O yr^{-1}, and for (b) the fast outflow, is $\geq 5x10^{-6}$ M_O yr^{-1}. "l-he disk mass is $\approx 6x10^{-3}$ M_O. The very fast optical outflow contains a mass of =7x10-4 M_O ejected at a rate of =5x10-7 M_O yr^{-1}. The kinetic temperature in the slow outflow lies in the range (20-70) K as a result of grain photoelectric heating,

5) Wc detected emission from ^{13}CO, as well as the high-excitation species HCN, CN, ^{13}CN, HCO^+, and 1113CO+, and possibly N_2H^+, in their 1-O transitions. The $^{13}C/^{12}C$ ratio is estimated to be 0.33. Both the HCO^+/HCN and CN/HCN line-intensity ratios are enhanced, the former by a very large factor, over the values found in the envelopes of AGB stars, probably as a result of enhancement of the CN and HCO^+ abundances due to photo-chemistry induced by the stellar UV. The CS J=2- 1, SiO J=2-1(v=0) and SiS J-6-5 lines were not detected to low levels.

6) In order to excite the rotational levels of the high-excitation molecules to detectable levels and to assure their survival against photodissociation by the UV radiation, significant clumping of the molecular gas into clumps with densities -few x 10^5 cm^{-3} is necessary.

7) The IRAS fluxes ofM1-16 imply the presence of about (1 .7-O.43)X 10^{-3} M_O of cool dust (temperature, T= 41-53K), and a smaller quantity, (2.7 -3.1)$x10^{-6}$ M_O of warmer dust (T= 114-13 1K) for a power-law emissivity index p=1 -2.

8) Single-star tracks for planetary nebula nuclei do not fit Ml -1 6's small evolutionary age of $\leq$850 yr, low effective temperature (34000 K), and very low luminosity (120 L_O). The obvious implication is that M 1-16 has evolved from (at least) a binary star. The very high $^{13}C/^{12}C$ ratio suggests a possible evolutionary connection between M 1-16 and the rare class of J-type silicate-carbon stars, which also have high $^{13}C/^{12}C$ ratios, and are thought to be binary systems with accretion disks.

Our study of M 1-16, while clear] y showing the wealth of precise information which can be extracted from single-dish molecular-line observations of planetary nebulae, also underscores the need for further observations, (a) at high-spatial resolution (1 -few arcsec) using millimeter-wave interferometers, and (b) of high-excitation line and continuum emission in the submillimeter wavelength range, which we aim to conduct in the near future. Several of the issues raised by the molecular-line observations of M 1-16 which wc have addressed in this paper, such as the necessity for the gas to be distributed in small clumps, both from excitation and survivability requirements, apply in a more general context to most planetary nebulae with detected molecular emission.

We thank P. Bouchet and N.S. van der Bliek for acquiring and reducing the near-IR photometric data, and the SEST staff for their support, George Bowen, Lee-Anne WillsOn, Mark Morris& Peter Wannier provided helpful comments. RS acknowledges support from the Swedish Naturvetenskapliga Forskningsrådet grant # 9098-312, the Jet Propulsion Laboratory, California Institute of Technology (under contract to the National Aeronautics and Space Administration), and the National Research Council (National Academy of Sciences).

Table 1.

Molecule/1.inc	Frequency MHz	Tmb K	$\int T_{mb}dV$ K km $s^{-1}(1\sigma)$	V_{exp} km s^{-1}	σ(rms) K	$3\sigma/\sqrt{N}$(a) K	Δν MHz
CO J=1-0	115271.2	0.45	12.3(0.18)[b]	21[b]	0.021	0.013	0.69
CO J=2-1	230538.0	1.5	55.2(0.14)[b]	22[b]	0.022	0.0094	0.69
^{13}CO J=1-0	110201.36	0.15	4.2(0.085)	19	0.01	0.0067	0.69
$C^{17}O$ J=1-0	112358.78[b]	...	..	...	0.0074	0.0048	0.69
$C^{18}O$ J=1-0	109782.1	...	...	...	0.0034	0.0023	0.69
HCO^+ J=1-0	89188.5	0.038	1.5(0,084)	27	0.0058	0.0050	1.38
$H^{13}CO^+$ J=1-0	86754.3	0.012	0.47(0.076)	27	0.0049	0.0042	1.38
HCN J=1-O	88631.6[c]	0.023	1.0(0.070)	25[d]	0.0045	0.0039	1.38
CN							
N=1-0(J=1/2-1/2)	113488-11352(F)	0.027[f]	2.1(0.13)	...	0.0080	0.011	2.76
N=1-0(J=3/2-1/2)	113123-113191[e]	..(g)	1.5(0.16)	...	0.0097	0.013	2.76
^{13}CN J=1-0	108631 -108796C)	0.014[h]	1.07(0.096)[h]	...	0.0039	0.0076	5.53
N_2H^+ J=1-O	93173.5	..(g)	0. 14(0.045)	...	0.01	0.0036	0.172
SiO J=2-1 (v=0)	86847.0			...	0.0049	0.0052	1.38
CS J=2-1	97980.97			...	0.016	0.011	0.69
SiS J=6-5	108924			...	0.004	0.0032	5.53

Notes

a) For each line, the number in this column multiplied by the total velocity range covered by the line, gives the statistical 3σ uncertainty (in K km s^{-1}) in the measured line flux ($\int T_{mb}dV$), since the line emission is spread over many spectrometer channels

b) Refers to the main profile, arising in the "slow" outflow, and excludes the contribution from weak line-wings, arising in a "fast" outflow.

c) Relative-intensity weighted mean frequency for line containing three hyperfine components

d) Expansion velocity derived from line after deconvolving hyperfine structure

e) Many hyperfine hyperfine components present in given frequency range

f) Several, but not all hyperfine components, contribute to peak intensity

g) The low signal-to-noise, together with the presence of several hyperfine components, prevents the determination of a meaningful peak line-intensity

h) Peak and integrated line-intensity derived for a "composite" line-profile produced by co-adding two sets of hyperfine components, centred at 108648 and 108784 MHz

Table 2

Data/ Model #	dM/dt (10^{-5} $M_O yr^{-1}$)	CO/H_2 (10^{-4})	1-0 (SEST) (K)	Cen. (K)	2-1 (s13s"1') 11 "/Cen. (K)	22"/Cen. (K)	2-1 (NRAO) Cen. (K)
Data . . .		...	0.45	1.75	0.58[a)]	o.13@	0.88
1	5.5	1.8	0.45	1,6	0.58	0,12	0.91
2	8.7	1	0.44	1.7	0.59	0.12	0.95

Notes.

a. Azimuthal average

Table 3

Molecule/Line	Abundance) (w.r.t. HCN)	Abundance[b)] (w.r.t. H_2)	Dipole Moment (Ref.) (Debyes)
HCN J=1-0	1.0	1. OX1O-7	2.98 (Tomasevich1970)
HCO^+ J=1-0	0.93	9.3 X1 0-8	4.07 (Haese & Woods 1979)
$H^{13}CO^+$ J=1-0	0.31	3.1 X1 0-8	4.07 (assumed same as HCO^+)
CN J=1-0	8.5	8.5x10-7	1.45 (Thomson & Dalby 1968)
^{13}CN J=1-0	2.7	2.7x10-7	1.45 (assumed same as CN)
N_2H^+ J=1-0	0.11	$1.1x10^{-8}$	3.4 (Green, Montgomery & Thaddeus 1974)
SiO J=2- 1 (v=0)	<0.24	<2.4x10-8	3.098 (Raymonda, Muenter, & Klemperer 1970)
SiS J=6-5	<0.42	<4.2x10-8	1.73 (Hoeft et al. 1969)
CS J=2- 1	<0.88	<8.8 X1 O-8	1.96 (Winnewisser & Cook 1968)

Notes.

a) The molecular abundances relative to HCN are rather insensitive to the value of the assumed excitation temperature, T_{ex}, and independent of R_{out} and dM/dt, except for SiS, where it scales as $(T_{ex})^{-0.6}$.

b) The molecular abundances relative to H_2 are $\propto$ "l'$_{ex}$a (1 5K<T_{ex}<60K), $\propto (R_{out})^{-2}$, and $\propto (dM/dt)^{-1}$, where a≈0.75, 0.69, and 0.1 respectively, for species in which the 1-0, 2-1, or 6-5 transition was observed. In the above table, we have assumed T_{ex}=15K, R_{out}=1.5x10] ^{7} cm, and dM/dt=$5.4x10^{-5}$ $M_O yr^{-1}$.

Table 4

Wavelength (microns)	Flux Jy	Reference
J	1.25x 10^{-2}±3.0x 10-4	this paper
H	4.87x 10-3*1.4x10-4	this paper
K	6.63x 10-3*3.3x10-4	this paper
I-	1.35x 10^{-2}±3.7x10^{-3}	this paper
12	0,3	IRAS
25	2.3	IRAS
60	9.2	IRAs
100	7.3	IRAS

References

Aaquist, O.B. and Kwok, S. 1990, A&A Suppl. Ser., 84, 229

Aspin, C., Schwarz, H.E., Smith, M.G. et al. 1993, A&A, in press

Bachiller, R., Huggins, P. J., Cox, P., and Forveille, T. 1993, A&A, 267, 177

Bachiller, R., Planesas, P., Martin-F) intado, J., Bujarrabal, V., Tafalla, M. 1989a, A&A, 210,366

Bachiller, R., Bujarrabal, V., Mar(in-Pintado, J., Gomez-Gonzalez, J. 1989b, A&A, 218, 252

Bergman, P., Carlström, U., and Olofsson, H. 1993, A&A, 268, 685

Bessel], M. S., Wood, P. R., and Lloyd Evans, 3'.1983, MNRAS, 202, 59

Bieging, J.H., Wilner, D., &Thronson, H.A. 1991, ApJ, 379, 271

Booth, R. S., Delgado, G., Hagström, M. et al. 1989, A&A, 216, 315

Bujarrabal, V., and Bachiller, R. 1991, A&A, 242,247

Cox, P., Omont, A., Huggins, P.J., Bachiller, R., and Forveille, T. 1992, A&A, 266,420

Deguchi, S., Izumiura, H., Kaifu, N., Mao, X., Nguyen-Q. -Rieu, Ukita, N. 1990, ApJ, 351, 522

Deguchi, S., Nakada, Y., and Sahai, R. 1990, A&A, 230, 339

Dominy, J.F. 1984, ApJ Suppl., 55, 27

Doyon, R., Puxley, P. J., Joseph, R. Il. 1992, ApJ, 397, 117

Dyson, J. E., Hartquist, T.W., Pettini, M., and Smith, L.J. 1989, MNRAS, 241, 625

Gerin, M., Combes, F., Encrenaz, P., Linke, R., Destombes, J.]., and Demuynck, C. 1984, A&A 136,1>17

Green, S., Montgomery (Jr.), J. A., & Thaddeus, P. 1974, ApJ (Letters), 193,1.89

Haese & Woods 1979, Chem. Phys. Lett. 61, 396

Healy, A.P. & Huggins, P.J. 1990, AJ, 100, 511

Hoeft, J., Lovas, F. J., Tiemann, E., and Torring, T. 1969, Z. Naturforsch. 24a, 1422

Hollenbach, D., Takahashi, T., and Tielens, A. G.G.M. 1991, ApJ, 377, 192

Howe, D. A., Millar, T. J., and Williams, D.A. 1992, MNRAS, 255,217

Huggins, P.J. and Healy, A.P. 1989, ApJ, 346, 201

Jaminet, P. A., Danchi, W. C., Sutton, E, C., Russell, A. P. G., Sandell, G., Bieging, J.H., Wilner, D. 1991, ApJ, 380, 461

Kahane, C., Cernicharo, J., Gonwz-Gonzalez, J., and Guélin, M. 1993, A&A, in press

Kwan, J., and Linke, R.A. 1982, ApJ, 254, 587

Lambert, D,],., Gustafsson, B., Eriksson, K., and Hinkle, K. II. 1986, ApJ Suppl. Ser. 62, 373

Lambert, D.L., Hinkle, K.H., and Smith, V. 1990, AJ, 99, 1612

Lloyd-Evans, T. 1990, MNRAS, 243, 336

Maroon, G. A., Glassgold, A.E., Huggins, P.J. 1988, ApJ, 328, 397

Morris, M., Guilloteau, S., Lucas, R., Omont, A. 1987, ApJ, 321,888

Pijpers, F.P. and Habing, H.J. 1989, A&A, 215, 334

Pijpers, F. P., Hearn, A, G., and Habing, H.J. 1990, in *From Miras to Planetary Nebulae: Which Path for Stellar Evolution? , eds.* M.O. Mennessier & A. Omont, Editions Frontieres, Paris, p. 131

Raymonda, W. A., Muenter, J. S., & Klemperer, W.A. 1970, J. Chem. Phys. 52, 3458

Richer, 11.13.1981, ApJ, 243,744

Sabbadin, F., Strafella, F., and Bianchini, A., A&A Suppl. Ser. 1986, 65, 259

Sahai, R. 1990, ApJ, 362, 652

Sahai, R., Wootten, A., and Clegg, R.E.S. 1990a, in *From Miras to Planetary Nebulae: Which Path for Stellar Evolution?,* eds. M.O. Mennessier & A. Omont, Editions Frontiers, Paris, p. 424.

Sahai, R., Wootten, A., and Clegg, R.E.S. 1990b, A&A, 234,1..1

Sahai, R., Wootten, A., Schwarz, H.E., and Clegg, R.E.S. 1991, A&A, 251, 560

Sahai, R., Wootten, A., and Clegg, R. E. S., IAU Symposium 155, *Planetary Nebulae,* eds. R. Weinberger and A. Acker (Dordrecht: Reidel) 1993, in press

Shaw, R. A., and Kaler, J.B. 1989, ApJ. Suppl. Ser. 69, 495

Schneider, S. E., Terzian, Y., Purgathofer, A., Perinotto, M. 1983, ApJ Suppl. Ser. 52, 399

Schwarz, H.E. 1992, A&A, 264, 1.1

Tomasevich, G. 1970, Thesis, Harvard University

Thomson, R. & Dalby, F.W. 1968, Canadian J. Phys, 46,2815

Truong-Bach, Morris, D., Nguyen-Q.-Rieu, and Deguchi, S. 1990, A&A, 230,431

Vorontsov-Velyaminov, B.A. 1968, in *Planetary Nebulae,* eds. D. Osterbrock and C. O'Dell (Reidel, Dordrecht), p. 256

Wannier, P.G., and Sahai, R. 1992, BAAS 24, 1179

Wannier, P.G., and Sahai, R. 1987, ApJ, 319, 367

Wegner, G., and Glass, I.S. 1979, MNRAS, 188, 327

Winncwisser, G.and Cook, R. I,. 1968, J. Mol. Spect. 28, 266

Wood, P. R., and Faulkner, D.J. 1986, ApJ, 307, 659

FIGURE CAPTIONS

1.The ^{12}CO J=2-1& 1-O, and ^{13}CO J=1-O spectra observed towards the center of M 1-16 (1950 RA=7h 34^m 55s.4, and DEC=-9° 32' 00") with the Swedish-llSO-Subnlillin~ ctcr-Telescope (SEST). The ^{12}CO J=2-1& 1-0 profiles have been displaced from the x-axis vertically by 1.OK and O. SK, respectively. 'l'he central component of the profile (31 km $s^{-1} \leq V_{LSR} \leq 69$ km s^{-1}) mostl y arises in a slow outflow, with V_{exp}= 19 km s^{-1}, whereas the weak emission in the wings, seen in both the ^{12}CO spectra, results from a high-velocity ouflow.

2. A composite CO J=2- 1 line profile generated by averaging all J=2-1 spectra offset by +/- 11" in RA and/or DEC from the center. Emission from the high-velocity outflow is more sensitively seen in this line profile than in the on-source profile.

3. Map of the CO J=2- 1 emission from M 1-16, made with 11" spacings.

4. CO J=2-1 emission intensity (integrated over discrete velocity intervals) mapped as a function of velocity. Panels are labelled from a) to f) for reference. As marked in panel (b), the x-axis shows the RA offset from source center, over the range -30" (right) to 30" (left), and the y-axis shows the DEC offset from source center, over the range -30" (bottom) to 30" (top). The lowest intensity contour is 1 K-km s-l, and the contour interval is 0,85 K-km s^{-1} in panels (a) and (f), and 1,7 K-km s^{-1} in panels b) through (e).

5. A difference spectrum, generated by subtracting an average of the S, SE, and E (O,- 11" = S, 11 ",-11" = SE, & 11",0= E) spectra from an average of the N, NW, and W (0,1 1" = N, -11 ",11" = NW and -11 ",0= W) spectra, in M 1-16. The spectrum clearly shows an "emission" peak 11 km s^{-1} bluewards, and an "absorption" peak at 11 km s^{-1} redwards, of the stellar velocity. The simplest explanation of this spectrum is that the emission in the <N, NW, W> and <S, SE, E> spectra contains contributions from opposite sides of an expanding disk-like structure which is inclined to the line-of-sight.

6, A schematic diagram of the various components of the composite molecular outflowinMl-16.

7. Spectra of the 1-O rotational transition of various molecular species observed in M 1-16 with the SEST. (a) HCO^+ (displaced vertically by 0.4 K), and H ^{13}CO, (b) HCN (c) CN (d) ^{13}CN (the insert shows a "composite" spectrum produced by co-adding the lower frequency set (average frequency, <v>=108648 MHz) and the higher freqency set (<v>=108784 MHz) of hyperfine components (e) N_2H^+. Vertical bars, with lengths proportional to the relative intensity of various hyperfine components, are marked at their center-frequencies in the HCN, CN, ^{13}CN, and N211+ spectra, Those components which are separated in frequency by less than half the channel spacing arc indicated as a single component.

Fig. 1.

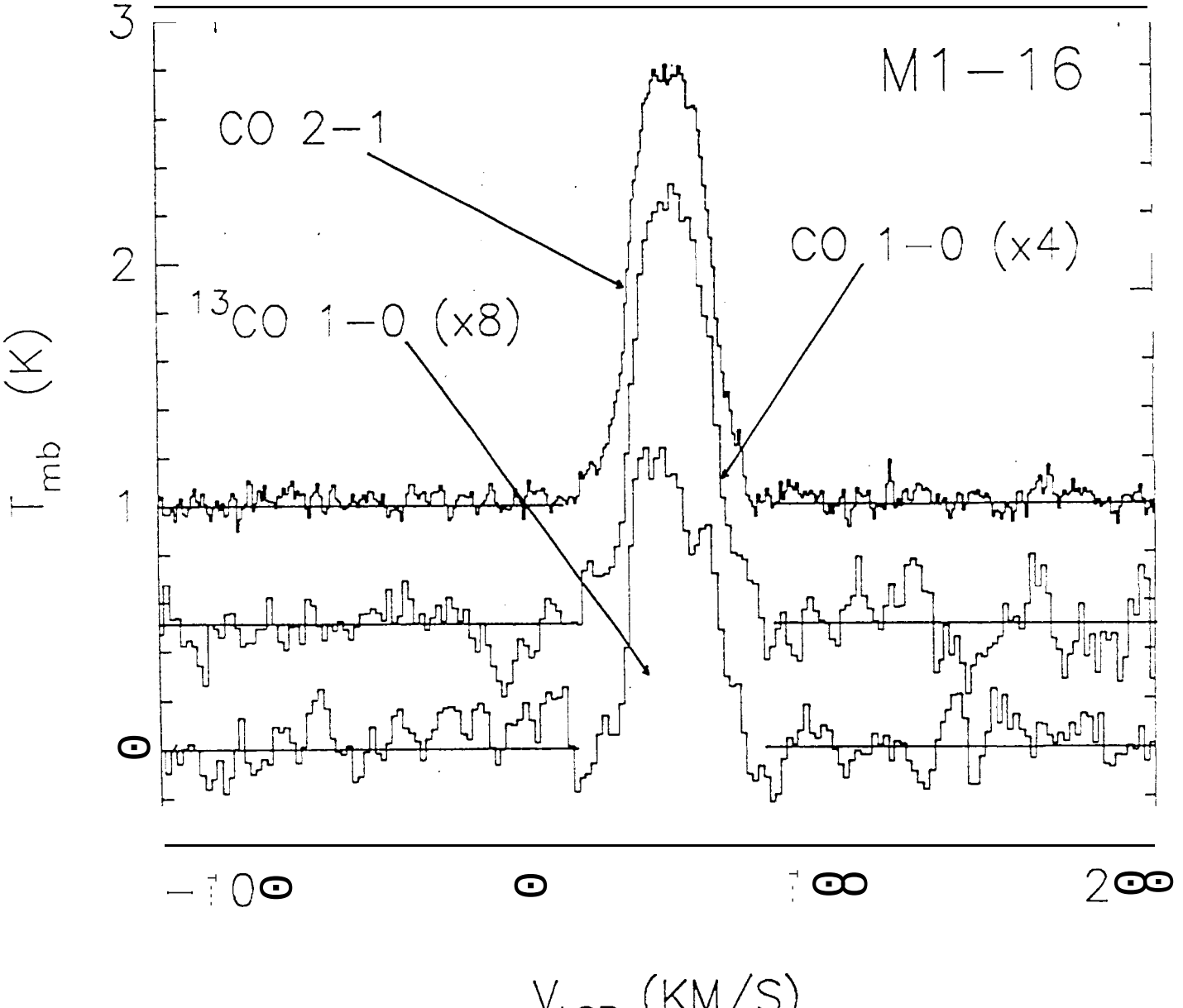

Fig 2.

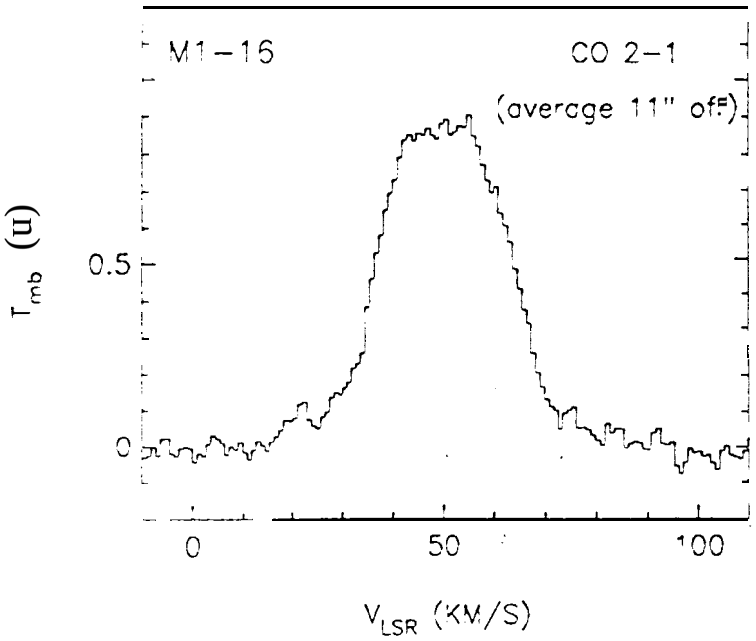

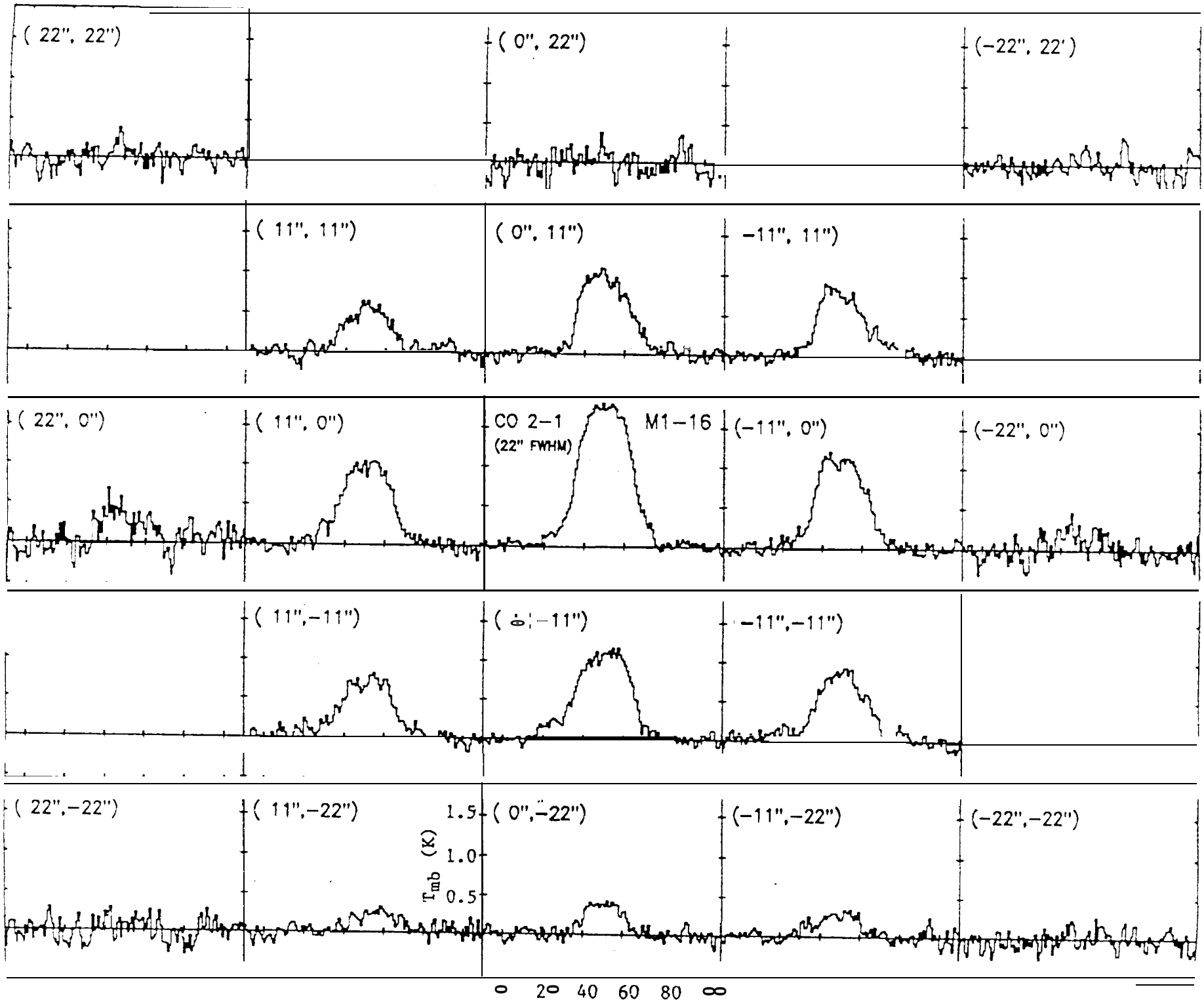
(22", 22")
(0", 22")
(−22", 22')
(11", 11")
(0", 11")
−11", 11")
(22", 0")
(11", 0")
CO 2−1
(22" FWHM)
M1−16
(−11", 0")
(−22", 0")
(11",−11")
(0",−11")
−11",−11")
(22",−22")
(11",−22")
(0",−22")
(−11",−22")
(−22",−22")
T_{mb} (K)
1.5
1.0
0.5
0
20
40
60
80

Fig. 4.

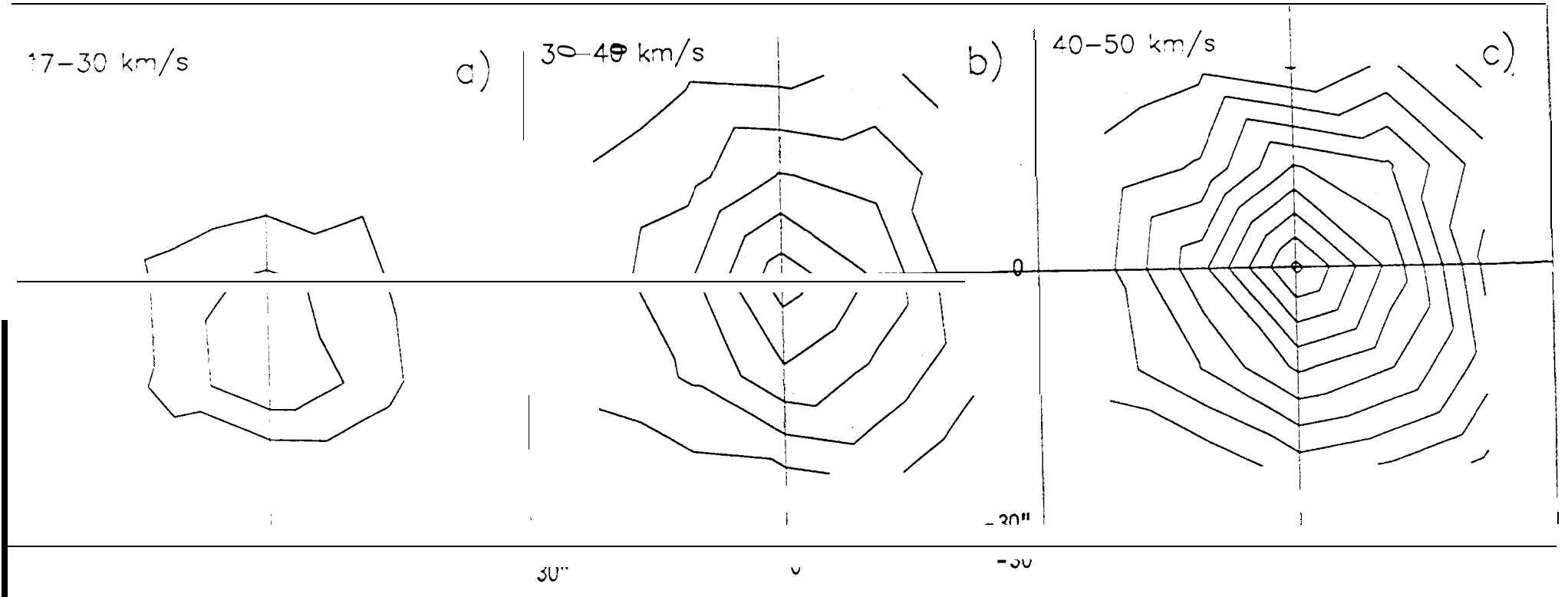
17–30 km/s
a)
30–40 km/s
b)
40–50 km/s
c)
0
-30"
30"
0
-30

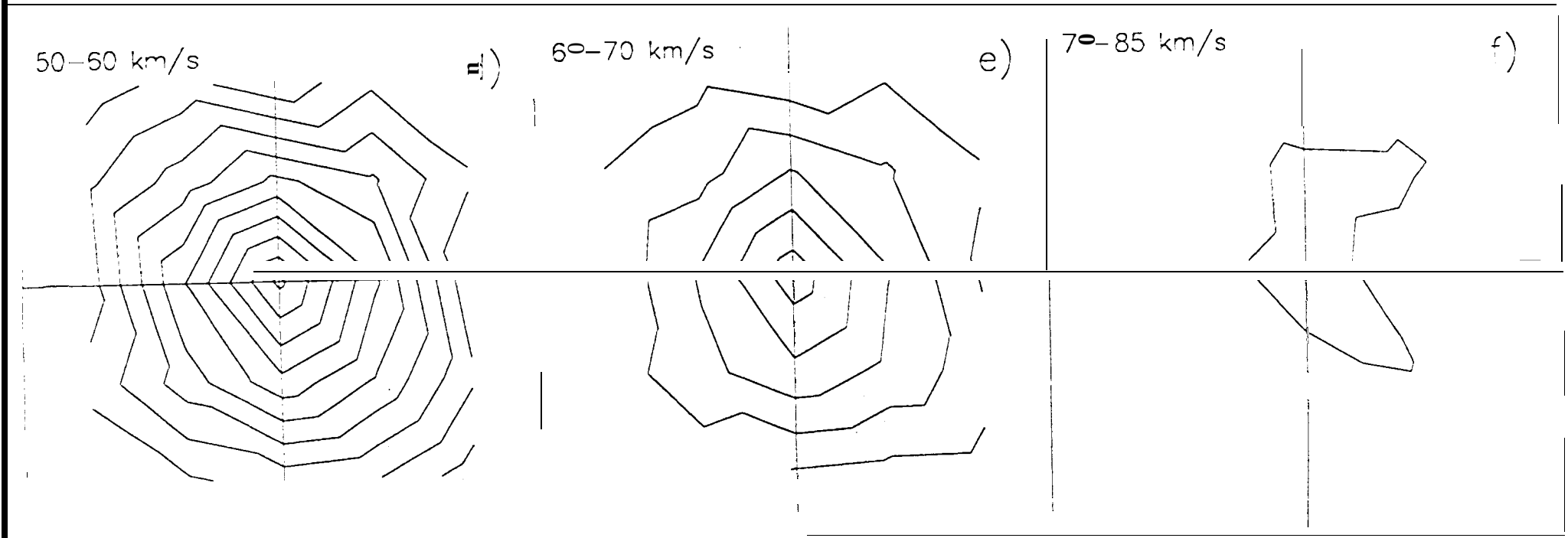
50–60 km/s
d)
60–70 km/s
e)
70–85 km/s
f)

Fig 5.

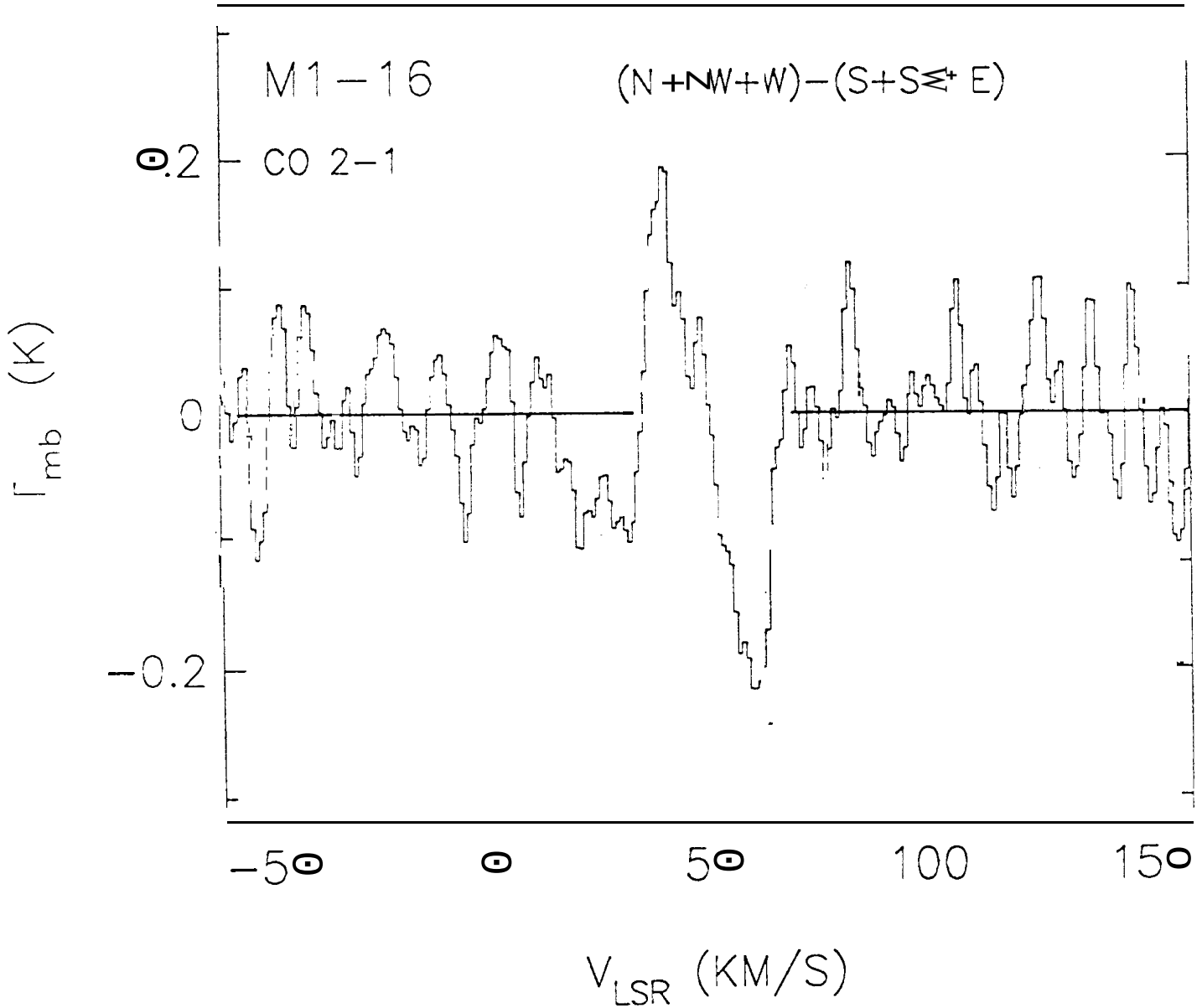

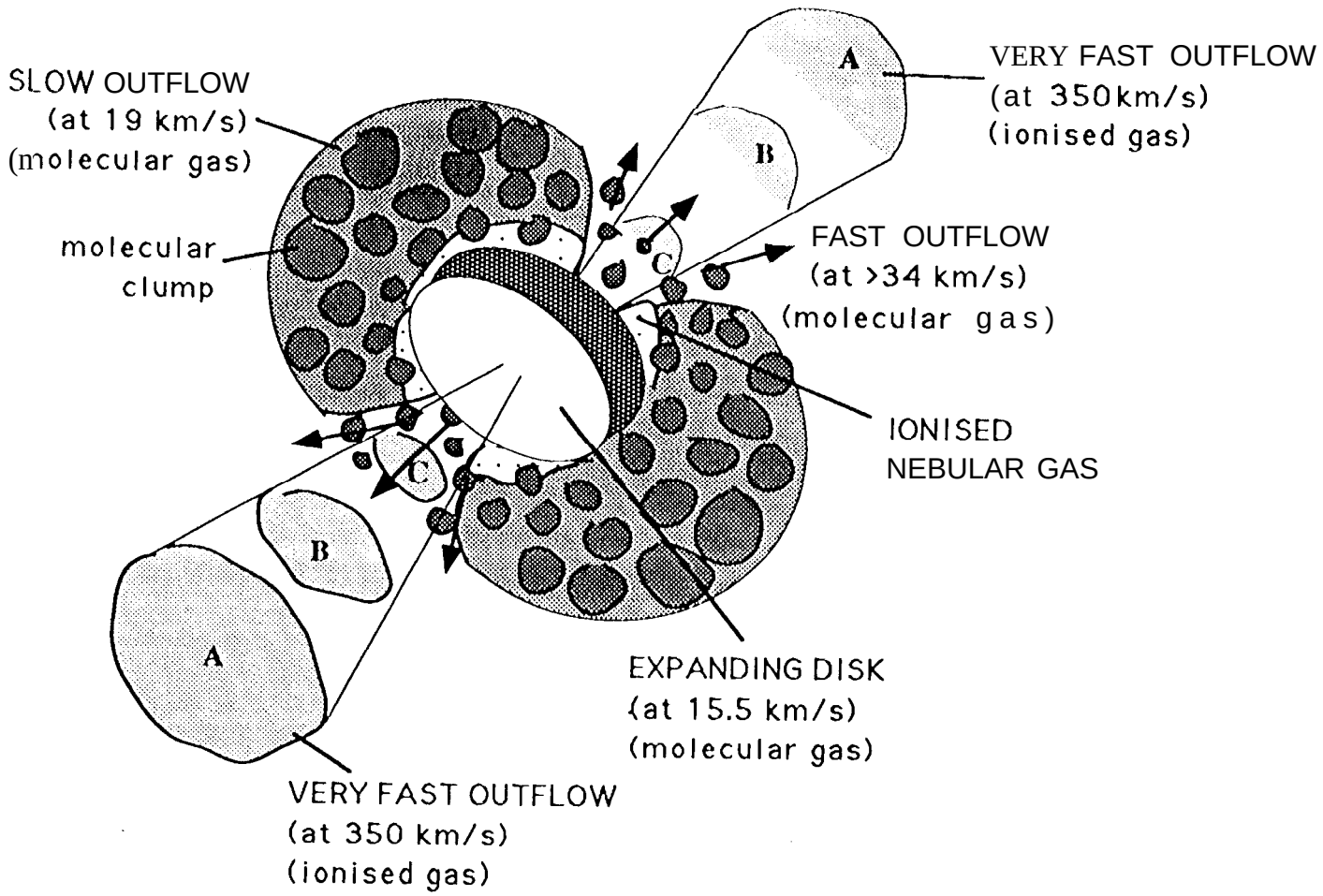
SLOW OUTFLOW
(at 19 km/s)
(molecular gas)
molecular
clump
A
B
C
VERY FAST OUTFLOW
(at 350km/s)
(ionised gas)
FAST OUTFLOW
(at >34 km/s)
(molecular gas)
IONISED
NEBULAR GAS
EXPANDING DISK
(at 15.5 km/s)
(molecular gas)
VERY FAST OUTFLOW
(at 350 km/s)
(ionised gas)

Fig. 6.

Fig. 7.(a)

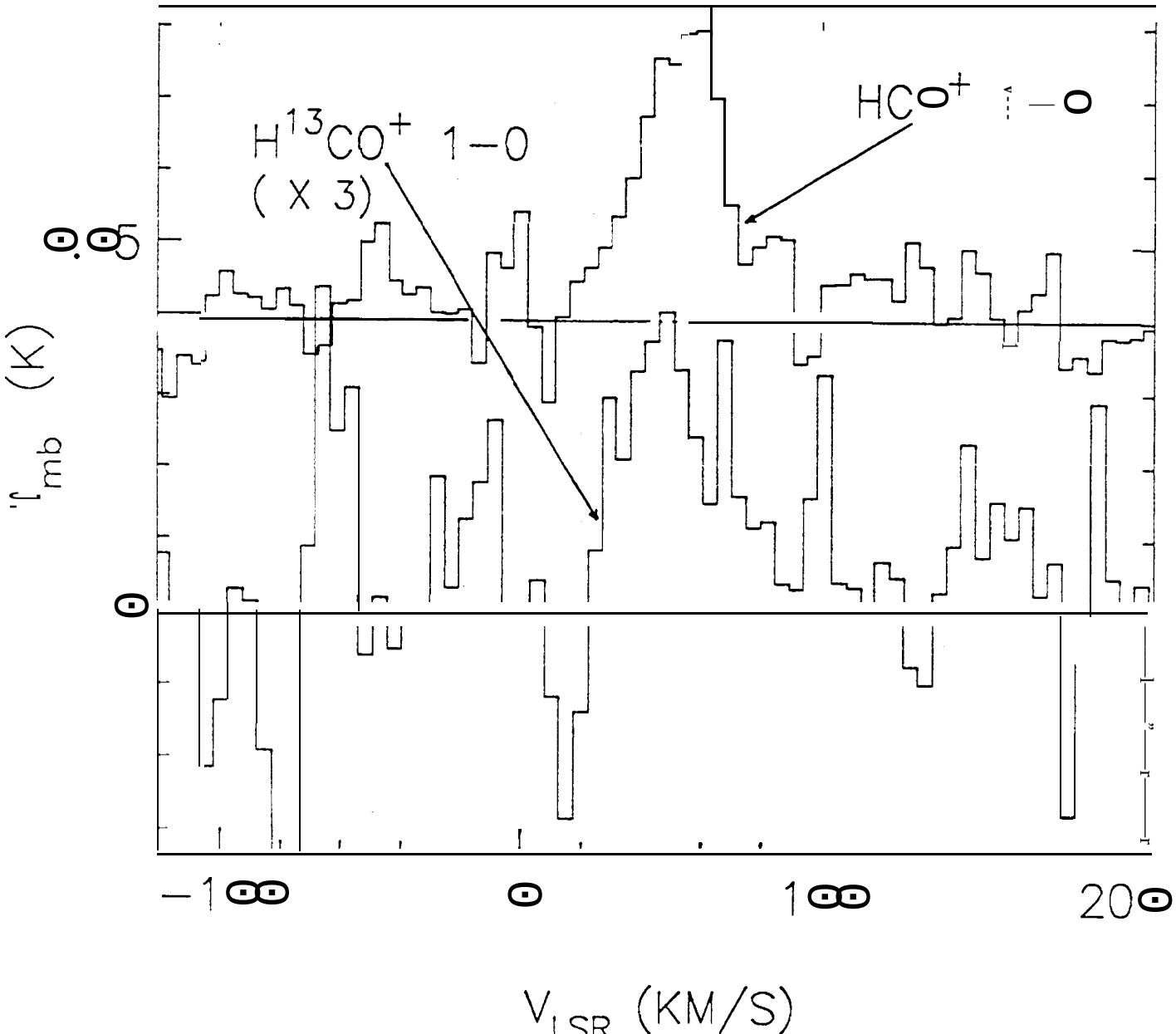

Fig. 7(b)

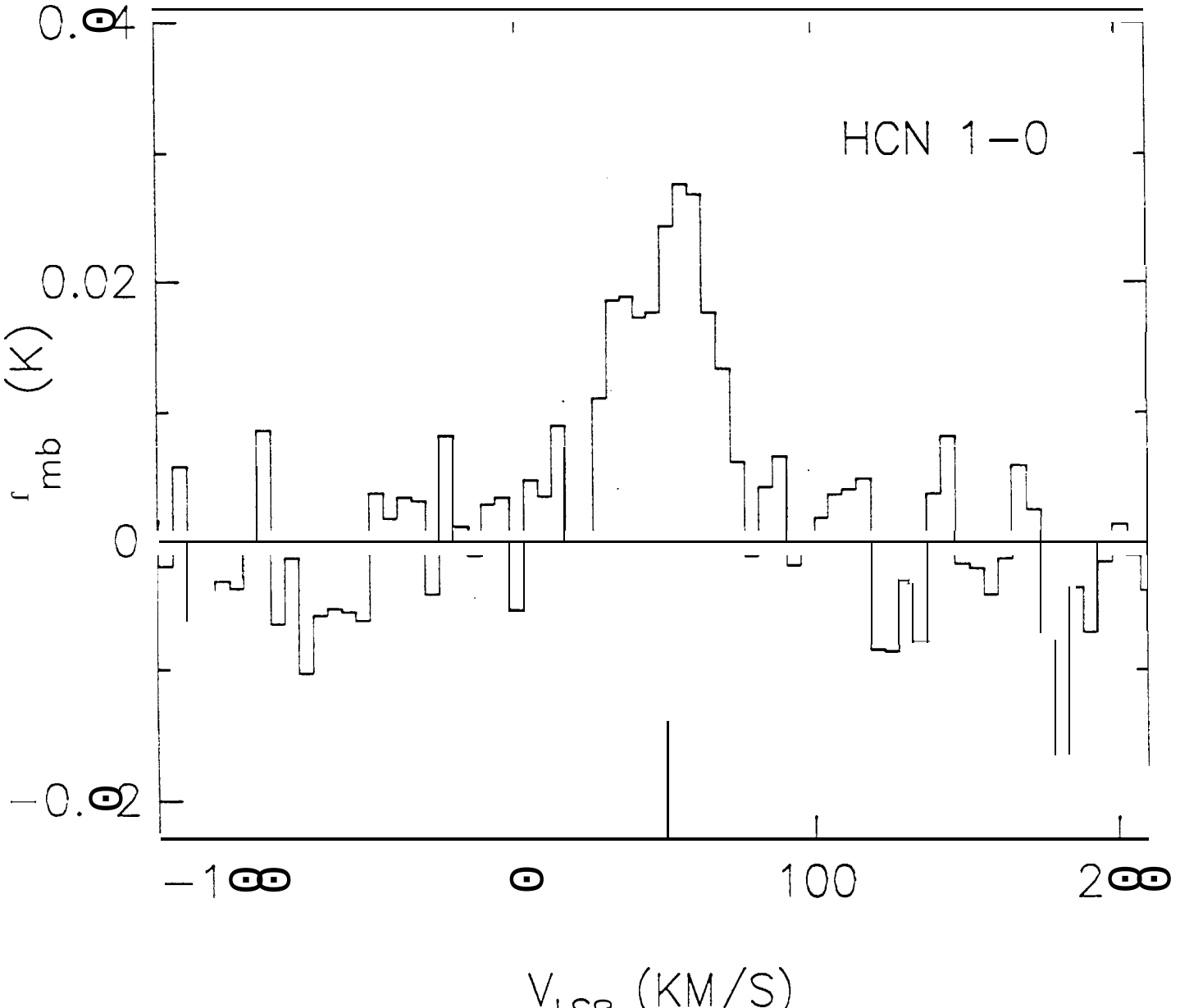

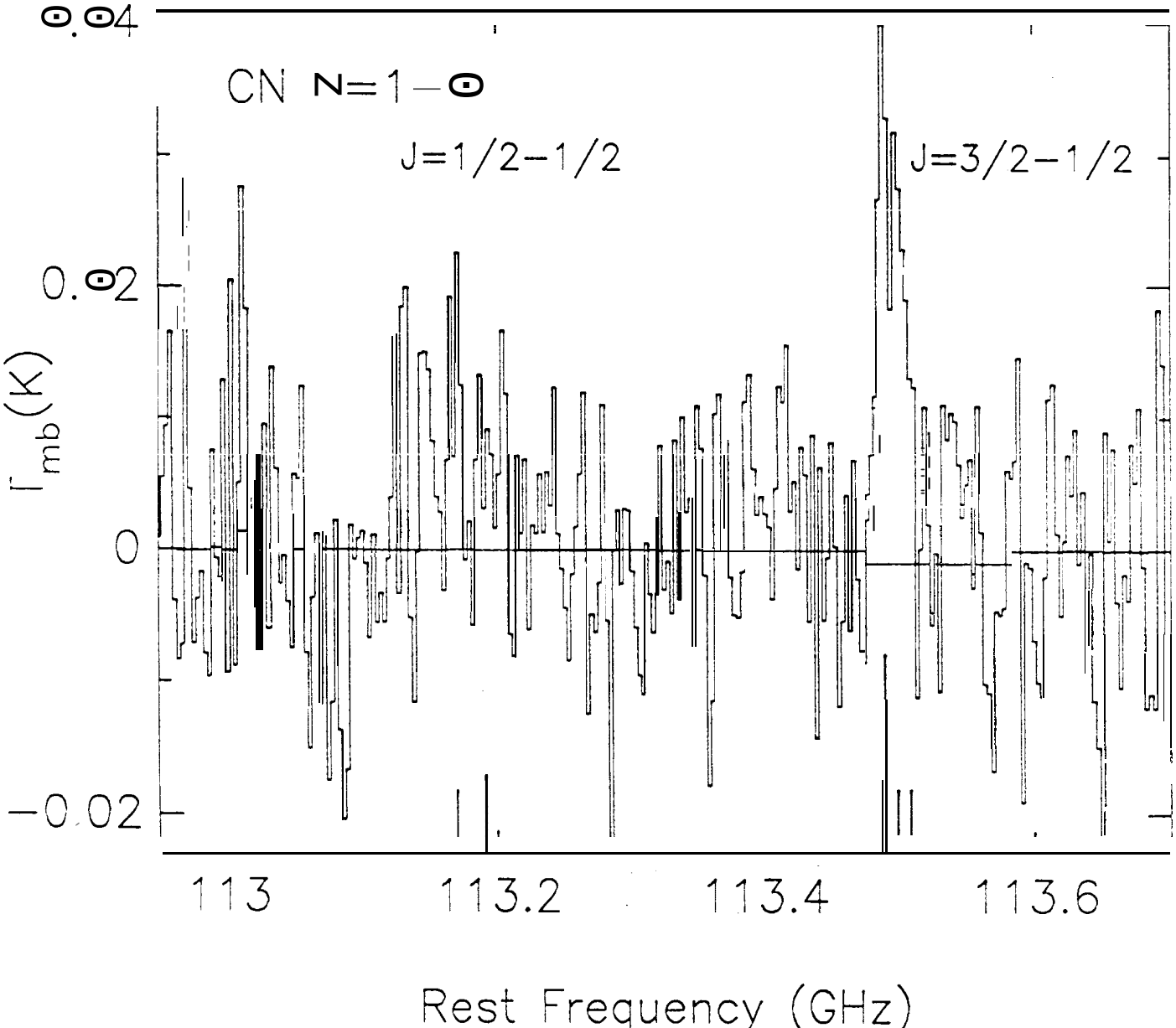
0.04
CN N=1−0
J=1/2−1/2
J=3/2−1/2
0.02
0
−0.02
T_{mb}(K)
113
113.2
113.4
113.6
Rest Frequency (GHz)

Fig. 7(d)

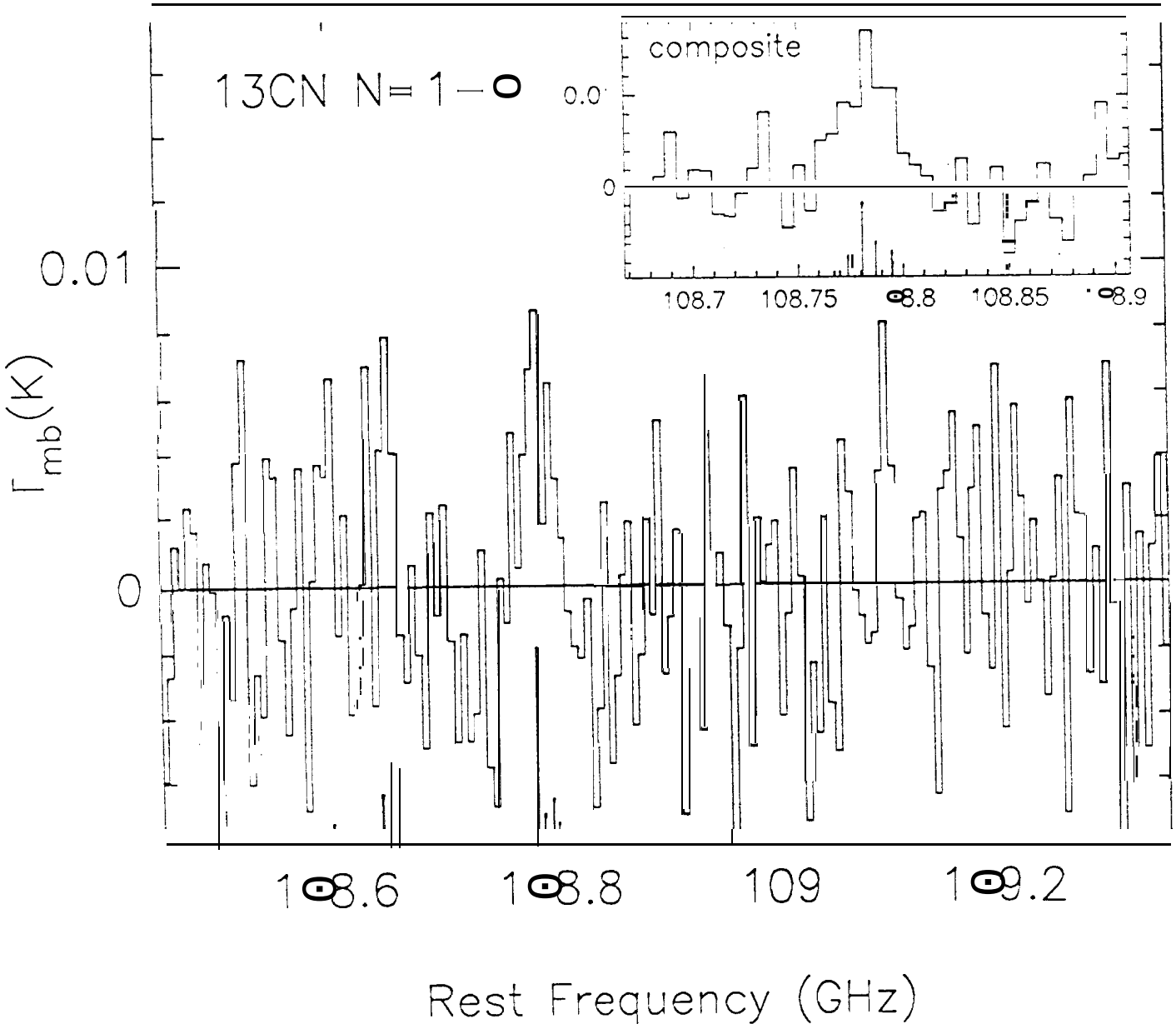
13CN N=1−0
composite
0.0
0
108.7
108.75
108.8
108.85
108.9
0.01
0
T_{mb}(K)
108.6
108.8
109
109.2
Rest Frequency (GHz)

Fig. 7(e)